nature cell biology

Endothelial adherens junctions control tight junctions by VE-cadherin-mediated upregulation of claudin-5

Andrea Taddei[1], Costanza Giampietro[1], Annarita Conti[1], Fabrizio Orsenigo[1], Ferruccio Breviario[2], Valentina Pirazzoli[1], Michael Potente[3], Christopher Daly[4], Stefanie Dimmeler[3] and Elisabetta Dejana[1,2,5,6]

Intercellular junctions mediate adhesion and communication between adjoining cells. Although formed by different molecules, tight junctions (TJs) and adherens junctions (AJs) are functionally and structurally linked, but the signalling pathways behind this interaction are unknown. Here we describe a cell-specific mechanism of crosstalk between these two types of structure. We show that endothelial VE-cadherin at AJs upregulates the gene encoding the TJ adhesive protein claudin-5. This effect requires the release of the inhibitory activity of forkhead box factor FoxO1 and the Tcf-4–β-catenin transcriptional repressor complex. Vascular endothelial (VE)-cadherin acts by inducing the phosphorylation of FoxO1 through Akt activation and by limiting the translocation of β-catenin to the nucleus. These results offer a molecular basis for the link between AJs and TJs and explain why VE-cadherin inhibition may cause a marked increase in permeability.

Endothelial cells (ECs) act as gatekeepers, controlling the infiltration of blood proteins and cells into the vessel wall. This unique characteristic is largely exerted by the coordinated opening and closure of cell–cell junctions[1]. Cell–cell junctions can also act as signalling structures that communicate cell position, limit growth and apoptosis and, in general, regulate vascular homeostasis[1,2]. Any change in junction organization might therefore result in complex consequences that compromise endothelial reactions with blood elements or modify the normal architecture of the vessel wall.

At both TJs and AJs, adhesion is mediated by transmembrane proteins that promote homophilic interactions and are linked inside the cells to specific intracellular partners that mediate their anchorage to the actin cytoskeleton. At AJs, adhesion is mediated by cadherins[1,2]; at TJs it is mediated by members of the claudin family[3]. ECs express cell-type-specific transmembrane adhesion proteins such as VE-cadherin at AJs[1] and claudin-5 at TJs[4].

Many reports have suggested that AJs and TJs are interconnected and that AJs influence TJ organization. Temporally, AJs precede TJs at intercellular contacts, and some TJ components such as ZO-1 and ZO-2 have been implicated in the crosstalk between these two junctional structures[5]. In addition, the nectin–afadin system participates in epithelial morphogenesis, cooperating with TJs and AJs[6].

In some, but not all, cell systems[7], blocking AJs inhibits the correct organization of TJs[8]. However, despite this indirect evidence, the molecular basis of AJ and TJ crosstalk is still unknown.

In ECs, there is a requirement for AJs (more specifically, VE-cadherin) for correct vascular development in the embryo. Genetic inactivation of VE-cadherin causes early embryo lethality at 9.5–10.0 days post coitum as a result of a lack of vascular remodelling[9]. In the adult, VE-cadherin-blocking antibodies induce a marked increase in vascular permeability[10]. Thus, VE-cadherin expression and organization at AJs is a crucial determinant for vascular stabilization.

Besides its adhesive properties, VE-cadherin acts by transferring intracellular signals. It can do this directly by engaging signalling proteins such as phosphatidylinositol-3-OH kinase (PI(3)K) or growth factor receptors, or indirectly by tethering and retaining transcription factors at the cell membrane such as β-catenin or p120^{ctn} and thereby limiting their translocation to the nucleus[11,12].

Here we describe a pathway through which VE-cadherin controls TJ organization. We found that VE-cadherin expression and clustering at junctions is required for the transcriptional upregulation of *claudin-5*. This effect is due to the inactivation of the forkhead box factor FoxO1 and β-catenin, which, through binding to the *claudin-5* promoter, inhibit transcription. VE-cadherin exerts a double effect: it inhibits FoxO1 by triggering PI(3)K activity and limits the translocation of β-catenin to the nucleus. This molecular mechanism releases *claudin-5* inhibition and allows its robust transcription.

RESULTS

VE-cadherin expression and clustering upregulate *claudin-5*

To identify genes regulated by VE-cadherin expression, we compared a mouse *VE-cadherin*-null cell line (VEC-null) with the same line reconstituted with *VE-cadherin* wild-type cDNA (VEC-positive). The morphological

[1]FIRC Institute of Molecular Oncology, 20139 Milan, Italy. [2]Mario Negri Institute for Pharmacological Research, 20156 Milan, Italy. [3]Molecular Cardiology, Department of Internal Medicine III, University of Frankfurt, 60590 Frankfurt am Main, Germany. [4]Regeneron Pharmaceuticals, Inc., Tarrytown, New York 10591, USA. [5]Department of Biomolecular Sciences and Biotechnologies, School of Sciences, University of Milan, 20133 Milan, Italy. [6]Correspondence should be addressed to E.D. (elisabetta.dejana@ifom-ieo-campus.it).

Received 23 April 2008; accepted 16 June 2008; published online 6 July 2008; DOI: 10.1038/ncb1752

© 2008 Macmillan Publishers Limited. All rights reserved.

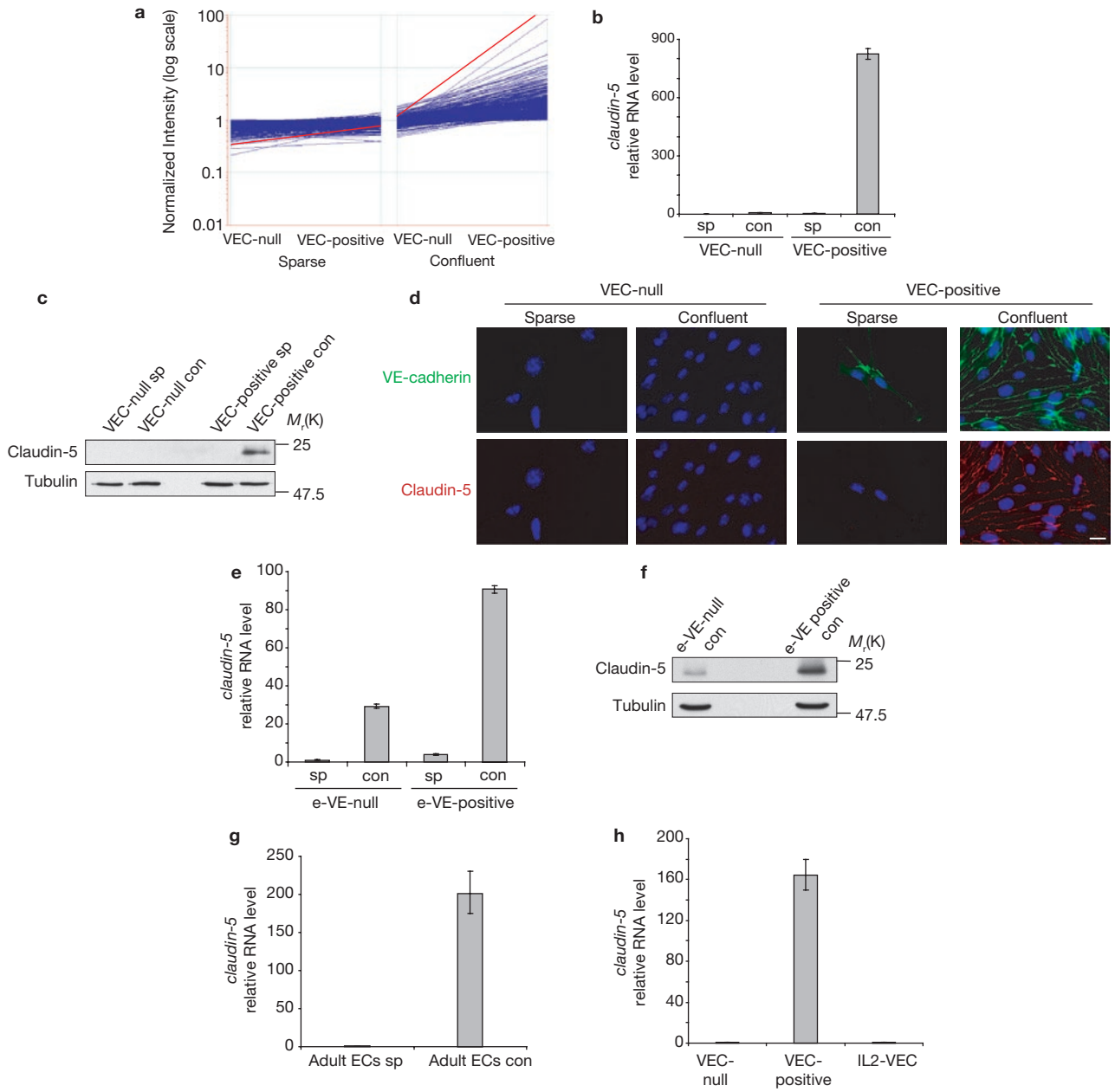

Figure 1 Claudin-5 is upregulated by VE-cadherin expression and clustering. (**a**) Graphical summary of Affymetrix analysis of genes upregulated in confluent VEC-positive cells. The red line refers to *claudin-5* gene expression. (**b**) Quantitative RT-PCR analysis of *claudin-5* expression in sparse (sp) and confluent (con) VEC-null and VEC-positive cells ($n = 6$). (**c**) Western blot analysis of claudin-5 in extracts of VEC-null and VEC-positive cells in sparse (sp) and confluent (con) conditions. Uncropped images of blots are shown in Supplementary Information, Fig. S7. (**d**) Immunofluorescence microscopy of VEC-null and VEC-positive cells in sparse and confluent conditions. Cells were double stained with anti-claudin-5 (red) and anti-VE-cadherin (green) antibodies. Junctional claudin-5 was detected only in confluent VEC-positive cells. Scale bar, 10 μm. (**e**) Quantitative RT-PCR analysis of *claudin-5* expression in sparse (sp) and confluent (con) e-VE-null and VEC-positive cells. (**f**) Western blot analysis of claudin-5 expression in extracts of e-VE-null and VEC-positive cells in the confluent condition. (**g**) Quantitative RT-PCR analysis of *claudin-5* expression in sparse (sp) and confluent (con) murine ECs derived from adult lung. (**h**) Quantitative RT-PCR analysis of *claudin-5* expression in confluent VEC-null, VEC-positive and IL2-VEC cells. In **b**, **e**, **g** and **h** the levels of mRNA are normalized to 18S; columns are means ± s.e.m. of triplicates from a representative experiment. In **e**, **g** and **h**, $n = 3$. The experiments reported in **c**, **d** and **f** were performed at least three times with comparable results.

and functional properties of these cell lines were described previously[13]. By Affymetrix gene expression analysis we found that, among the genes upregulated by VE-cadherin, *claudin-5* reached remarkably high levels (Fig. 1a). Full *claudin-5* upregulation required not only VE-cadherin expression but also cell confluence (Fig. 1a, compare VEC-positive in sparse or confluent conditions), suggesting that clustering of VE-cadherin at junctions was needed. Data were validated by quantitative real-time PCR (qRT-PCR; Fig. 1b), western blot analysis (Fig. 1c) and immunofluorescence (Fig. 1d).

Comparable results were obtained by using another EC line (e-VE-null) reconstituted, as above, with *VE-cadherin* cDNA (e-VE-positive) (Fig. 1e, f), and adult ECs from mouse lung in sparse and confluent conditions (Fig. 1g).

© 2008 Macmillan Publishers Limited. All rights reserved.

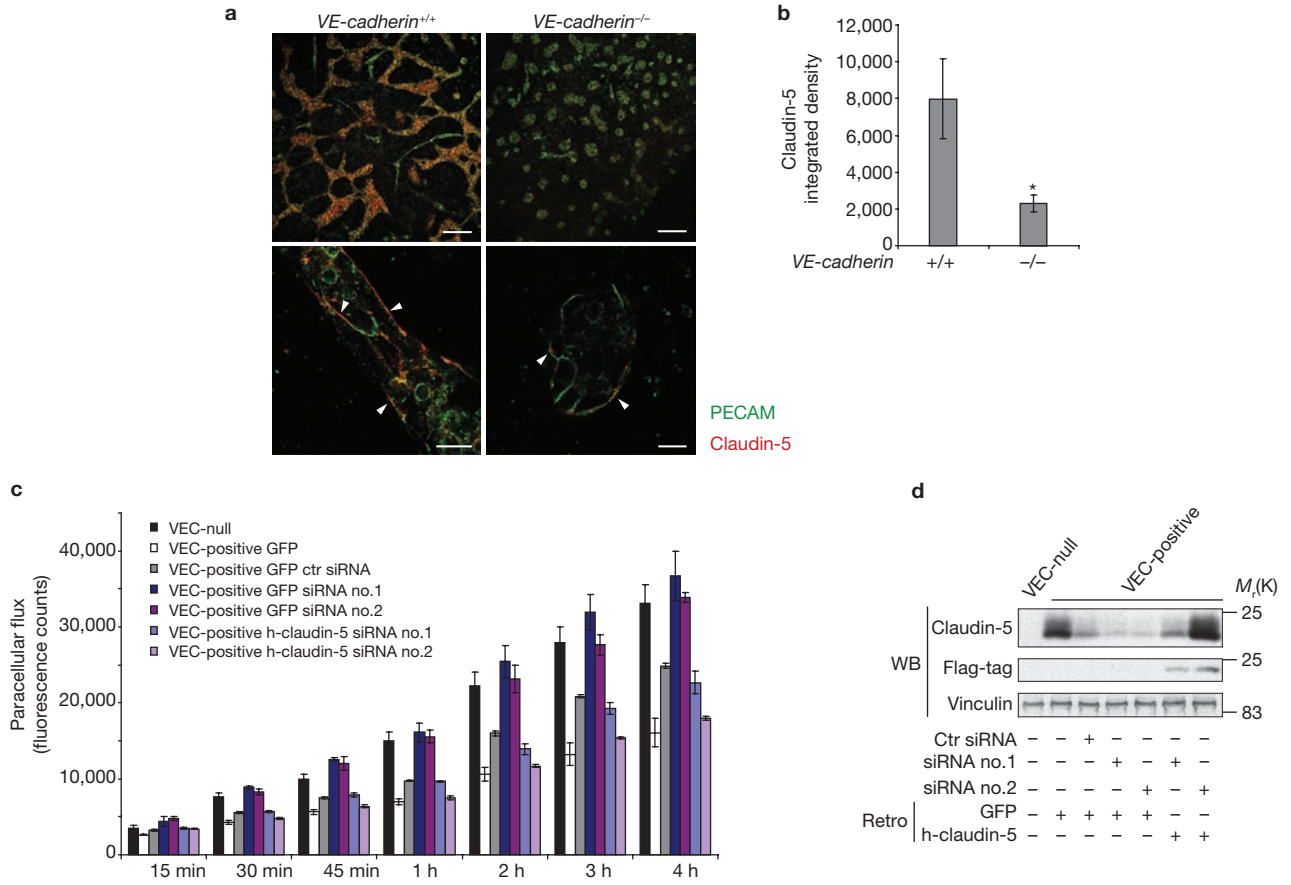

Figure 2 Claudin-5 upregulation by VE-cadherin in mouse allantoises and its role in the control of endothelial permeability. (**a**) Allantois organ culture assay. Allantoises obtained from *VE-cadherin*$^{+/+}$ and *VE-cadherin*$^{-/-}$ mice were cultured *ex vivo* for 48 h and then stained with anti-claudin-5 (red) and anti-PECAM (green) antibodies. Arrowheads point to claudin-5 distribution (note the junctional localization in *VE-cadherin*$^{+/+}$ allantoises and the dot-like distribution in *VE-cadherin*$^{-/-}$ allantoises). Scale bars, 100 μm (upper panels) and 10 μm (lower panels). (**b**) Quantification of claudin-5 fluorescence signal in *VE-cadherin*$^{+/+}$ and *VE-cadherin*$^{-/-}$ allantoises from confocal microscopy images performed with ImageJ 1.33. Data are means ± average deviation (a.d.; *t*-test: $^{*}P < 0.01$, *t*-test). (**c**) Paracellular tracer flux assay. VEC-positive cells were first infected with retroviral vectors to stably overexpress GFP or Flag-tagged h-claudin-5, then transfected either with control non-targeting siRNA (ctr siRNA) or two different anti-mouse *claudin-5* siRNAs (siRNA no. 1 and siRNA no. 2). Permeability to FITC-dextran (38 kDa) was assayed. Data are means ± s.e.m. of triplicates from a representative experiment out of three performed. At all time values from 30 min onwards, VEC-positive GFP, VEC-positive GFP ctr siRNA, VEC-positive h-claudin-5 siRNA no. 1 and VEC-positive h-claudin-5 siRNA no. 2 were statistically lower than VEC-null (analysis of variance and Dunnet test: $P < 0.01$–0.05). (**d**) Western blot (WB) analysis of total claudin-5 protein and Flag-tagged h-claudin-5 expression in extracts of VEC-null and VEC-positive cells overexpressing GFP or h-claudin-5 and transfected either with ctr siRNA or with siRNA no. 1 and siRNA no. 2. Knockdown of *claudin-5* in VEC-positive GFP siRNA no. 1 and siRNA no. 2 cells is shown. Note the weaker Flag-tag signal in VEC-positive h-claudin-5 siRNA no. 1 cells, probably due to the interference of siRNA no. 1 with the overexpressed h-claudin-5. Vinculin is shown as loading control. Retro, retroviral delivery. The experiments reported in these figure were performed at least three times with comparable results.

The need for VE-cadherin clustering to induce *claudin-5* upregulation was confirmed by expressing, in confluent VEC-null cells, a mutated version of VE-cadherin (IL2-VEC cells) made up of the VE-cadherin cytoplasmic domain fused to the extracellular and transmembrane domains of the interleukin-2 receptor α-chain. This VE-cadherin mutant is unable to cluster at junctions, although it still retains the capacity to associate with VE-cadherin cytoplasmic partners[14,15]. Confluent IL2-VEC cells proved unable to upregulate *claudin-5* (Fig. 1h), confirming the requirement for VE-cadherin clustering for *claudin-5* upregulation.

Upregulation of claudin-5 by VE-cadherin was also evident *ex vivo* in freshly isolated allantois organ culture[16] (Fig. 2a). Wild-type allantoises developed a well-defined network of vessels in which claudin-5 was highly expressed at cell contacts (Fig. 2a, lower left panel, arrowheads). Conversely, *VE-cadherin*-null allantoises had less organized vessels and a very low expression of claudin-5 (Fig. 2a, lower right panel, arrowheads, and Fig. 2b).

VE-cadherin controls vascular permeability *in vitro* and *in vivo*[9,10,17]. This effect was abrogated by mouse *claudin-5* knockdown *in vitro* and was rescued by expressing human claudin-5 (h-claudin-5; Fig. 2c). Moreover, we observed an inverse relationship between the level of claudin-5 protein expression (Fig. 2d) and the permeability of the EC layer. VEC-positive *h-claudin-5* short interfering RNA (siRNA) no. 1 cells expressed lower levels of total claudin-5 protein, probably because of some interference of siRNA no. 1 with h-claudin-5 (see the weaker Flag-tag signal in Fig. 2d) and showed a less complete rescue of the permeability phenotype. Knockdown of *claudin-5* did not grossly alter the junctional localization of VE-cadherin (Supplementary Information, Fig. S1), supporting the idea of a specific role of this protein in permeability control.

© 2008 Macmillan Publishers Limited. All rights reserved.

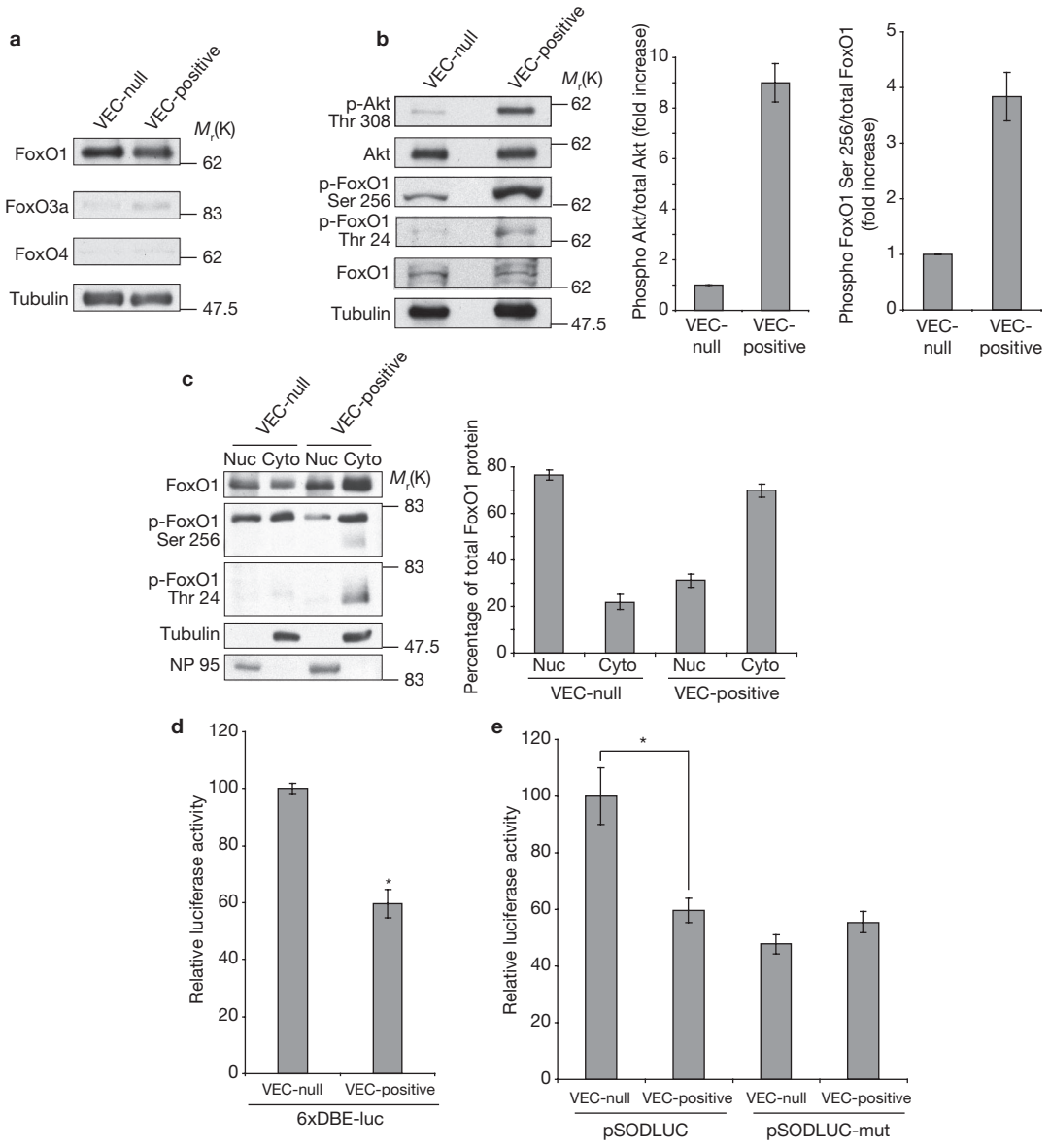

Figure 3 VE-cadherin activates the PI(3)K–Akt pathway and induces FoxO1 phosphorylation. (**a**) Western blot analysis of FoxO1, FoxO3a and FoxO4 in total cell lysates of confluent VEC-null and VEC-positive cells. The experiment was performed three times with comparable results. (**b**) Akt and FoxO1 phosphorylation (p-Akt Thr 308 and p-FoxO1 Ser 256 and Thr 24, respectively) in confluent VEC-null and VEC-positive cells. Cells were grown to confluence and then starved for 72 h. Total cell lysates were analysed by western blotting for phosphorylated and total Akt and FoxO1 expression by using specific antibodies. The graphs represent the western blot quantification. Columns are means ± s.e.m. of five independent experiments. Uncropped images of blots are shown in Supplementary Information, Fig. S7. In **a** and **b** tubulin was used as a loading control. (**c**) Nuclear/cytoplasmic distribution of FoxO1 in confluent VEC-null and VEC-positive cells. On VE-cadherin expression, FoxO1 shifted from a preferentially nuclear to a preferentially cytoplasmic localization. A strong FoxO1 phosphorylation at Thr 24 was detected only in the cytoplasmic fraction of VEC-positive cells, which is consistent with nuclear exclusion. Columns are means ± s.e.m. of three independent experiments. Tubulin and NP 95 were used as cytoplasmic and nuclear markers, respectively. Uncropped images of blots are shown in Supplementary Information, Fig. S7. (**d**) FoxO transcriptional activity. VE-cadherin expression determined a significant decrease in FoxO transcriptional activity, as measured by the luciferase reporter 6×DBE-luc vector. (**e**) FoxO transcriptional activity. The pSODLUC/pSODLUC-mut luciferase reporter system confirmed the results shown in **d**. The activity of the pSODLUC-mut control did not vary on VE-cadherin expression and clustering. In **d** and **e** data are means ± s.e.m. of six replicates from a representative experiment of three performed (*$P < 0.01$, *t*-test).

The effect of VE-cadherin seems to be specific for claudin-5 because by Affymetrix, immunofluorescence, qRT-PCR and western blot analysis the expression of other TJ constituents, including both transmembrane proteins (JAM A, B and C, claudin-3 and claudin-12) and intracellular partners (cingulin, ZO-1), was not significantly modified by VE-cadherin expression (Supplementary Information, Fig. S2a, b, and data not shown).

VE-cadherin clustering inhibits FoxO1 through the activation of the PI(3)K–Akt pathway

We next aimed at identifying the pathway through which VE-cadherin expression and clustering regulate claudin-5. In a microarray gene expression screening, *claudin-5* was found to be one of the genes downregulated by a constitutively active form of the transcription factor FoxO1 (ref. 18).

© 2008 Macmillan Publishers Limited. All rights reserved.

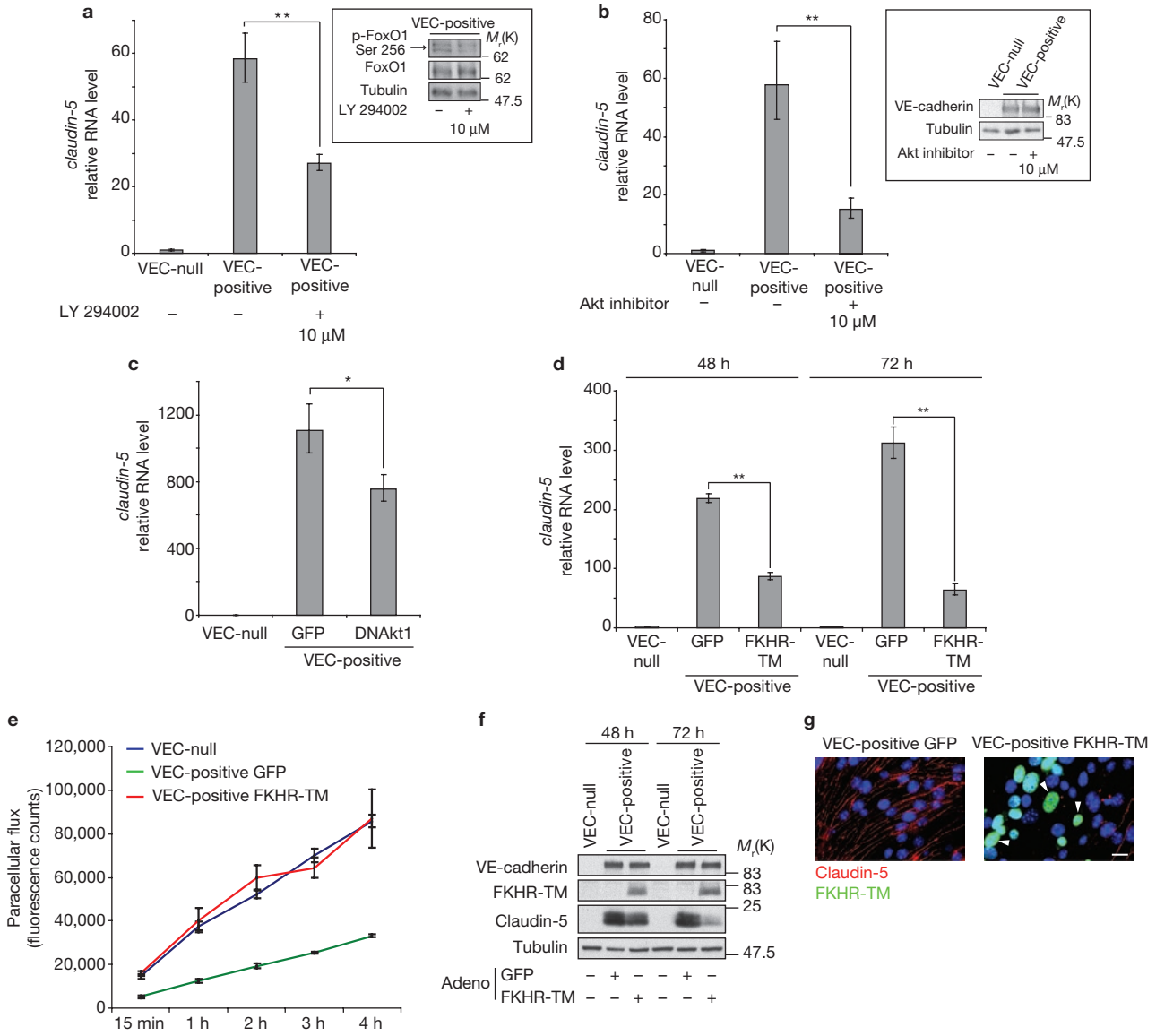

Figure 4 FoxO1 is a repressor of claudin-5 expression. (**a**) RT-PCR analysis of *claudin-5* on inhibition of PI(3)K. Cells were grown to 90% confluence, starved for 24 h and incubated overnight in complete medium with the PI(3)K inhibitor LY 294002 (10 μM). Inset: western blot analysis of p-FoxO1 Ser 256 and total FoxO1. (**b**) Quantitative RT-PCR analysis of *claudin-5* on inhibition of Akt. Cells were cultured as described in **a** and then incubated for 8 h in complete medium with the Akt inhibitor (10 μM). Inset: no alteration of VE-cadherin protein expression was observed on treatment with Akt inhibitor. (**c**) Quantitative RT-PCR analysis of *claudin-5* expression on overexpression of DNAkt1. VEC-positive cells were infected either with a control GFP retroviral vector or with a bicistronic one coding for both DNAkt1 and GFP (see Supplementary Information, Fig. S5d). Cells were grown to confluence, starved for 24 h and assayed for *claudin-5* expression. In **a** and **b** the levels of mRNA are normalized to 18S, and in **c** to β_2-microglobulin; columns are means ± s.e.m. of triplicates from a representative experiment out of at least three performed (*$P < 0.05$, **$P < 0.01$, *t*-test). (**d**) Expression of *claudin-5* after infection with FKHR-TM adenoviral vector. To limit the pro-apoptotic effect of FKHR-TM, cells were cultured after infection in the presence of the pan-caspase inhibitor zVAD-fmk (50 μM). RT-PCR was performed 48 and 72 h after infection. The levels of mRNA are normalized to GAPDH, columns are means ± s.e.m. of triplicates from a typical experiment ($n = 3$; **$P < 0.01$, *t*-test). (**e**) Paracellular tracer flux assay. Permeability to FITC-dextran (38 kDa) was assayed 72 h after adenoviral infection. Data are means ± s.e.m. of triplicates from a representative experiment ($n = 2$). (**f**) Protein expression of VE-cadherin, FKHR-TM (Myc-tag) and claudin-5 in confluent VEC-positive cells 48 and 72 h after infection with adenoviral vectors. Adeno, adenoviral delivery. (**g**) Immunofluorescence analysis of claudin-5 (red) and FKHR-TM (Myc-tag) (green) in confluent VEC-positive cells 72 h after infection, performed on Transwell Permeable Support membranes of **e**. Arrowheads point to cells positive for nuclear FKHR-TM expression. None of these cells showed junctional claudin-5. Scale bar, 10 μm. In **f** and **g** $n = 3$.

FoxO1 is phosphorylated and inactivated by PI(3)K–Akt[19], a pathway also triggered by VE-cadherin clustering[9]. We therefore examined whether VE-cadherin might upregulate *claudin-5* by inactivating FoxO1.

Consistently with other ECs[20], among the members of the FoxO subgroup (FoxO1, 3a and 4) the EC lines used here express FoxO1 preferentially (Fig. 3a and Supplementary Information, Fig. S3a). Immunoblotting analysis showed that VE-cadherin expression led to a ninefold increase in Akt phosphorylation (Fig. 3b). The robust activation of the Akt pathway was accompanied by FoxO1 phosphorylation at Ser 256, which blocks its binding to DNA, and at Thr 24, which

© 2008 Macmillan Publishers Limited. All rights reserved.

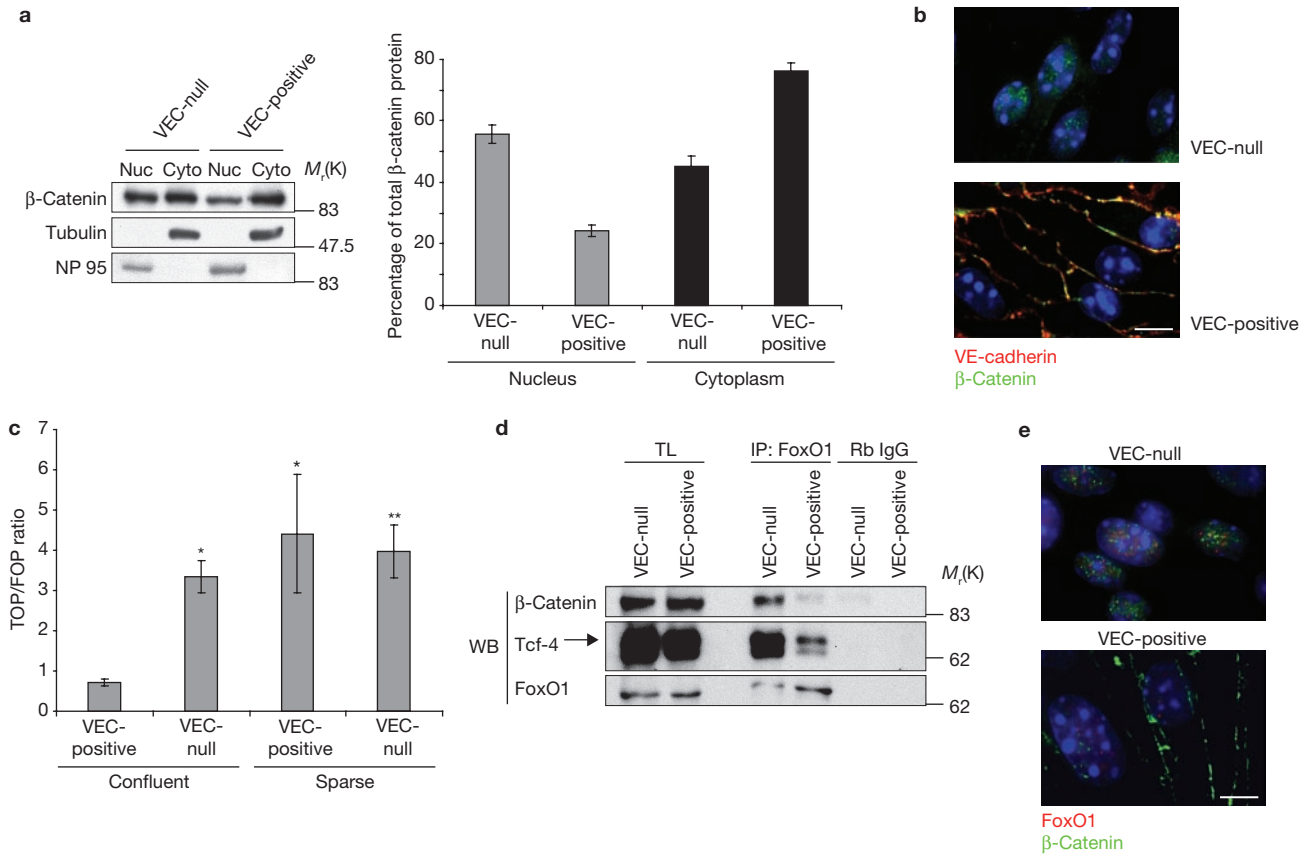

Figure 5 VEC-null cells present higher nuclear β-catenin localization, signalling and association with FoxO1. (**a**) Nuclear/cytoplasmic fractionation of confluent VEC-null and VEC-positive cells. The nuclear localization of β-catenin was decreased twofold in VEC-positive cells. Columns are means ± s.e.m. of three independent experiments. Tubulin was used as a cytoplasmic marker, NP 95 as a nuclear marker. Uncropped images of blots are shown in Supplementary Information, Fig. S7. (**b**) Immunofluorescence analysis of VE-cadherin (red) and β-catenin (green) expression and localization in confluent VEC-null and VEC-positive cells. Cells were grown to confluence and then starved overnight in the presence of LiCl (60 mM) to stabilize endogenous β-catenin, and in the presence of leptomycin B (10 ng ml^{-1}) to prevent the exit of β-catenin from the nucleus to the cytoplasm. VE-cadherin expression and clustering determined a redistribution of β-catenin from the nucleus to the plasma membrane. Scale bar, 5 μm. (**c**) Tcf–β-catenin transcriptional activity. The activity was determined by transfecting sparse/confluent VEC-null and VEC-positive cells with TOP/FOP constructs. Columns are means ± average deviation (a.d.) of triplicates from a representative experiment of three performed (*t*-test: $*P < 0.05$; $**P < 0.01$). (**d**) Association of β-catenin and Tcf-4 with FoxO1. Co-immunoprecipitation (IP) and western blot (WB) of endogenous β-catenin, Tcf-4 and FoxO1 from nuclear extracts of confluent VEC-null and VEC-positive cells. TL, total cell lysate. Uncropped images of blots are shown in Supplementary Information, Fig. S7. (**e**) Immunofluorescence analysis of FoxO1 (red) and β-catenin (green) expression and localization in confluent VEC-null and VEC-positive cells. Cells were cultured as described for **b**. VE-cadherin expression and clustering caused β-catenin redistribution to the plasma membrane and a decrease in FoxO1 nuclear localization. Scale bar, 5 μm. The experiments in **b**, **d** and **e** were performed at least twice with comparable results.

promotes its exclusion from the nucleus[19,21,22] (Fig. 3b, c). Consistently, in confluent VEC-null cells FoxO1 was preferentially localized in the nucleus, whereas in the presence of VE-cadherin it was shifted to the cytoplasmic fraction (Fig. 3c). A strong Thr 24 phosphorylation of FoxO1 was detected only in the cytosolic fraction of confluent VEC-positive cells (Fig. 3c). Consistently, the activation of Akt and phosphorylation of FoxO1 induced by VE-cadherin expression was also much higher in confluent cells than in sparse cells (Supplementary Information, Fig. S3b). Transfection of FoxO reporter plasmids (6×DBE-luc or pSOD-LUC) in confluent VEC-positive and VEC-null cells revealed a significant decrease in luciferase expression in VEC-positive ECs (Fig. 3d, e). These reporter plasmids proved sensitive to endogenous FoxO1 because the knockdown of the transcription factor led to a consistent decrease in their reporter activity (Supplementary Information, Fig. S3c–e).

Consistently with the observed regulation of FoxO1 activity, the expression of several FoxO1-upregulated target genes (*Bcl-2-interacting mediator of cell death* (*bim*)[23], *vascular cell adhesion molecule 1* (*VCAM1*)[24], *vascular endothelial growth factor (VEGF)-receptor 1* (ref. 18) and *sprouty2* (ref. 24)) was significantly higher in confluent VEC-null cells than in VEC-positive cells (Supplementary Information, Fig. S2c).

It has been reported that ECs are able to express VEGF-A endogenously[25]. Given the association of VE-cadherin with VEGF-receptor 2 in confluent VEC-positive cells[9], we checked whether activation of Akt by VE-cadherin clustering was due to changes in VEGF signalling. Confluent VEC-positive cells were treated with DC101 antibody[26], which prevents VEGF-receptor 2 stimulation by binding to the growth-factor-binding pocket (Supplementary Information, Fig. S4a, b) or with sunitinib malate (SU11248), a chemical inhibiting VEGF-receptor 2 tyrosine kinase activity[27] (Supplementary Information, Fig. S4c, d). No changes in Akt phosphorylation and claudin-5 expression were observed. We conclude that the activation of the Akt pathway induced by VE-cadherin clustering is independent of VEGF signalling.

© 2008 Macmillan Publishers Limited. All rights reserved.

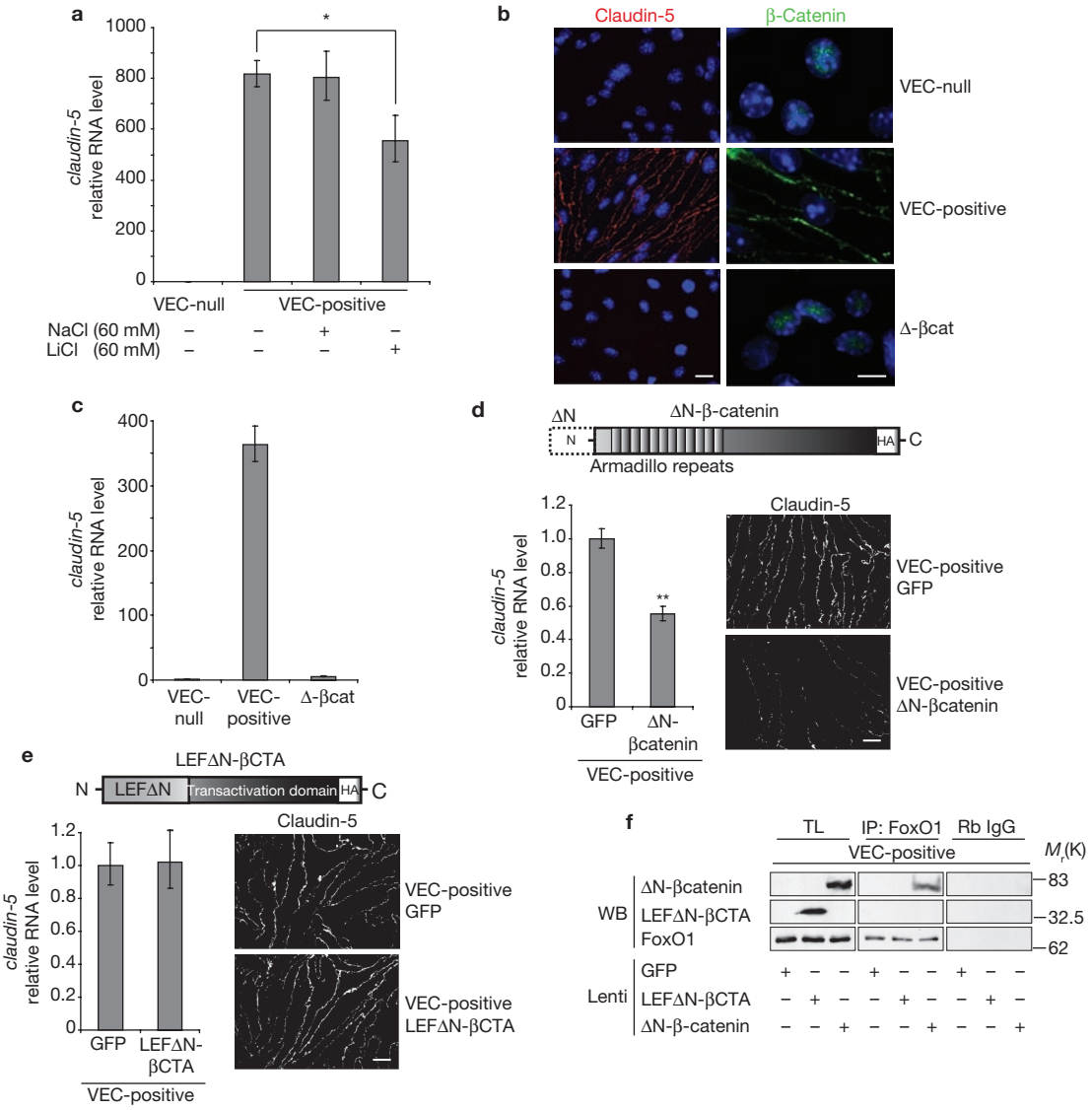

Figure 6 β-Catenin association enhances FoxO1 repressor activity on claudin-5 expression. (**a**) Quantitative RT-PCR analysis of *claudin-5* expression after cell treatment with LiCl. Endogenous β-catenin in confluent VEC-positive cells was stabilized by overnight treatment with LiCl (60 mM). NaCl (60 mM) was used as a control for non-specific osmotic effects. (**b**) Immunofluorescence analysis of confluent VEC-null, VEC-positive and Δ-βcat cells stained with anti-claudin-5 (red, left panels) and anti-β-catenin (green, right panels) antibodies. Scale bars, 10 μm (left panels) and 5 μm (right panels). (**c**) Quantitative RT-PCR of *claudin-5* expression performed on confluent VEC-null, VEC-positive and Δ-βcat cells. (**d**) Effect of ΔN-βcatenin mutant on claudin-5 expression. VEC-positive cells were infected with ΔN-βcatenin (upper panel) or control GFP lentiviral vectors, grown to confluence, and claudin-5 expression was evaluated by quantitative RT-PCR (left panel) and immunofluorescence analysis (right panel). Scale bar, 10 μm. (**e**) Lack of effect of LEFΔN-βCTA mutant on claudin-5 expression. VEC-positive cells were infected with LEFΔN-βCTA (upper panel) or control GFP lentiviral vectors and grown to confluence; claudin-5 expression was evaluated by quantitative RT-PCR (left panel) and immunofluorescence analysis (right panel). Scale bar, 10 μm. In all RT-PCR analyses reported in the figure, the levels of mRNA are normalized to 18S; columns are means ± s.e.m. of triplicates from a typical experiment of three performed (*$P < 0.05$, **$P < 0.01$, *t*-test). (**f**) Association of endogenous FoxO1 with ΔN-βcatenin but not with LEFΔN-βCTA. Co-immunoprecipitation between endogenous FoxO1 and ΔN-βcatenin or LEFΔN-βCTA mutants from nuclear extracts of confluent VEC-positive cells infected with β-catenin mutants or control GFP lentiviral vectors. TL, total cell lysate; Lenti, lentiviral delivery. The experiment was performed three times with comparable results. Uncropped images of blots are shown in Supplementary Information, Fig. S7.

Thus, VE-cadherin expression and clustering activate the Akt pathway, which in turn induces the phosphorylation of FoxO1 and the inhibition of its transcriptional activity.

VE-cadherin clustering induces *claudin-5* upregulation through inhibition of FoxO1 transcriptional activity

We then investigated whether FoxO1 is a transcriptional repressor of *claudin-5*. First, to increase the transcriptional activity of endogenous FoxO1, we treated VEC-positive ECs with the PI(3)K inhibitor LY 294002. As a consequence of the decreased phosphorylation of FoxO1 (Fig. 4a inset), we observed a significant downregulation of *claudin-5* expression (Fig. 4a), although AJ organization was not affected (Supplementary Information, Fig. S5a). Similar results were obtained by treating the cells with an Akt inhibitor (Fig. 4b and Supplementary Information, Fig. S5b). The overexpression of a dominant-negative form of Akt1 (DNAkt1)[28] (Fig. 4c), the major Akt isoform expressed in ECs, as well as siRNA-mediated *Akt1*

© 2008 Macmillan Publishers Limited. All rights reserved.

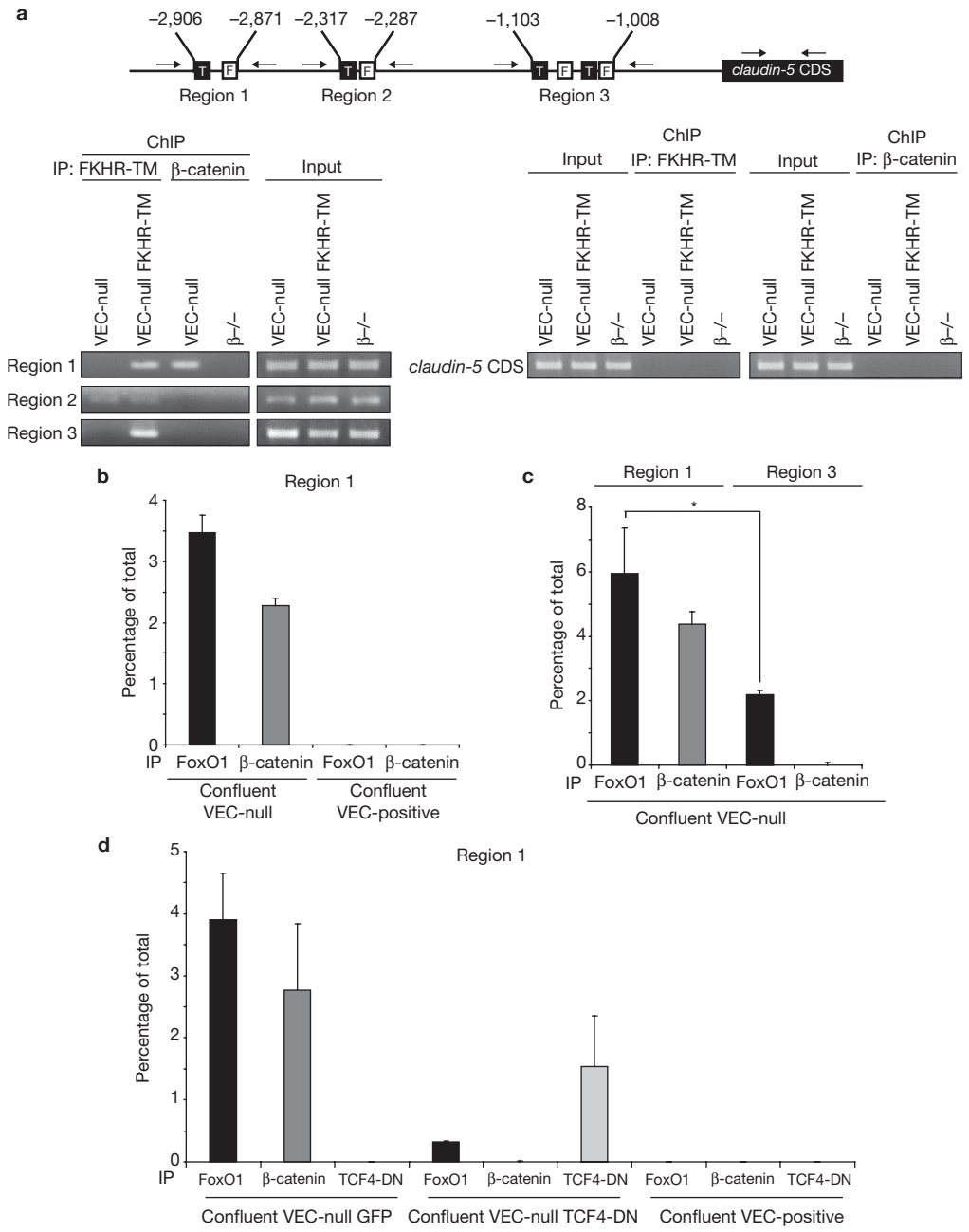

Figure 7 FoxO1 and β-catenin bind to *claudin-5* promoter region. (**a**) ChIP assay of the putative promoter region of the *claudin-5* gene (upper panel). To check for FoxO1 binding to DNA, confluent VEC-null cells were infected with Myc-tagged FKHR-TM adenoviral vector. At 24 h after infection, FKHR-TM-bound chromatin was immunoprecipitated (IP) with anti-Myc-tag antibody. For β-catenin, chromatin from confluent VEC-null cells was immunoprecipitated with anti-β-catenin antibody (lower panel). Confluent uninfected VEC-null and confluent β-catenin (β–/–) cells were used as negative controls for FoxO1 and β-catenin ChIP, respectively. Primers for the *claudin-5* CDS were used as a negative control to exclude non-specific precipitated DNA. T, Tcf–β-catenin-binding site; F, FoxO binding site; CDS, coding sequence. (**b**) Quantitative RT-PCR for Region 1 performed on endogenous FoxO1- and β-catenin-bound chromatin immunoprecipitated from confluent VEC-null and VEC-positive cells. (**c**) Quantitative RT-PCR for Regions 1 and 3 performed on endogenous FoxO1- and β-catenin-bound chromatin immunoprecipitated from confluent VEC-null cells. (**d**) Quantitative RT-PCR for Region 1. Confluent VEC-null cells were infected with control GFP or TCF4-DN adenoviral vectors and analysed 24 h after infection. Quantitative RT-PCR was performed on FoxO1-, β-catenin- and TCF4-DN-bound chromatin immunoprecipitated from confluent VEC-null GFP, VEC-null TCF4-DN and VEC-positive cells. In **b**, **c** and **d** the levels of DNA are normalized to input, columns are means ± s.d. of triplicates from a representative experiment ($n = 3$; $^*P < 0.05$, *t*-test).

knockdown (Supplementary Information, Fig. S5c) led to a significant decrease in claudin-5 expression.

Next, we infected confluent VEC-positive cells with adenoviruses encoding either green fluorescent protein (GFP) or a constitutively active form of FoxO1 (FKHR-TM or triple mutant) in which the three Akt-phosphorylation sites (Ser 256, Thr 24 and Ser 319) were changed to alanine to prevent inhibition by the Akt pathway[18]. Expression of FKHR-TM led to a strong downregulation of claudin-5 at both the mRNA level and the protein level (Fig. 4d, f). Cell infection with this construct was higher than 50%, and, by immunofluorescence, cells positive for

© 2008 Macmillan Publishers Limited. All rights reserved.

FKHR-TM were invariably negative for claudin-5 (Fig. 4g, arrowheads). As a consequence of claudin-5 downregulation, the permeability of VEC-positive FKHR-TM cells was strongly increased (Fig. 4e). We conclude that FoxO1 is a transcriptional repressor of the *claudin-5* gene in ECs.

β-Catenin binds FoxO1 and increases its repressor activity

A recent study reported an evolutionarily conserved functional interaction between FoxO transcription factors and β-catenin. This association leads to an increase in FoxO transcriptional activity[29].

We therefore tested whether β-catenin might contribute to VE-cadherin-mediated claudin-5 regulation. It was proposed that VE-cadherin, by recruiting β-catenin at the plasma membrane, might control its nuclear translocation and transcriptional activity[21,30]. To assess this possibility in our system, we compared VEC-positive and VEC-null cells for the nuclear localization and transcriptional signalling of β-catenin. We found that nuclear β-catenin levels in confluent VEC-null cells were double those in VEC-positive cells (Fig. 5a). Immunofluorescence analysis clearly showed a redistribution of β-catenin from the nucleus to the plasma membrane on VE-cadherin expression and clustering (Fig. 5b). Consistently, β-catenin transcriptional activity, detected by a Tcf luciferase reporter, was significantly lower in confluent VEC-positive cells than in VEC-null or sparse cells (Fig. 5c).

We then checked whether β-catenin could associate with FoxO1. Co-immunoprecipitation from nuclear extracts showed that β-catenin and Tcf-4 associate with FoxO1 and that the complex was much more abundant in VEC-null cells than in VEC-positive cells (Fig. 5d). Immunofluorescence staining showed a higher nuclear level of FoxO1 and nuclear localization of β-catenin in VEC-null cells (Fig. 5e), which is consistent with the observed greater association between these two molecules.

To assess the role of β-catenin in claudin-5 downregulation, we stabilized β-catenin by treating confluent VEC-positive cells with the glycogen synthase kinase 3β (GSK3β) inhibitor LiCl. Under these conditions *claudin-5* expression was significantly decreased (Fig. 6a). Comparable data were obtained by the lentivirus-mediated expression of ΔN-βcatenin, a stabilized form of the molecule lacking the GSK3β phosphorylation site (see below, Fig. 6d).

Furthermore, the role of VE-cadherin in recruiting β-catenin at the membrane was assessed by reconstituting VEC-null cells with a truncated mutant of VE-cadherin lacking the β-catenin-binding domain (Δ-βcat)[13]. In these cells, VE-cadherin was unable to sequester β-catenin at the membrane and to increase claudin-5 expression (Fig. 6b, c).

Taken together, these findings favour the notion that nuclear β-catenin contributes to claudin-5 downregulation. However, it was not clear whether this effect required the direct interaction of β-catenin with FoxO1. To clarify this point we infected VEC-positive cells with lentiviral vectors coding for the LEFΔN-βCTA mutant[31], consisting of the DNA-binding region of LEF1 fused to the transactivation domain of β-catenin, and ΔN-βcatenin, a stabilized form of the molecule lacking the GSK3β phosphorylation site. Both mutants have transcriptional activity, but only ΔN-βcatenin expresses the armadillo repeats and is able to interact with FoxO1 as reported in Fig. 6f. Only ΔN-βcatenin-infected VEC-positive cells showed a downregulation of claudin-5, whereas no effect was observed on the expression of LEFΔN-βCTA (Fig. 6d, e). We conclude that the regulation of claudin-5 expression requires a direct interaction between β-catenin and FoxO1.

Using the 6×DBE-luc reporter plasmid[20] we analysed FoxO1 transcriptional activity in confluent VEC-positive cells expressing LEFΔN-βCTA and ΔN-βcatenin mutants. The reporter plasmid contains six FoxO-binding sites but no sites for the binding of Tcf–β-catenin. No change in FoxO1 activity was detected in the presence of β-catenin mutants (Supplementary Information, Fig. S6). Thus, the binding of both Tcf–β-catenin and FoxO1 to DNA is required for their cooperative action to occur. These data also exclude the possibility that Tcf–β-catenin exerts an indirect effect on FoxO1 activity or stability, independent of interaction with DNA.

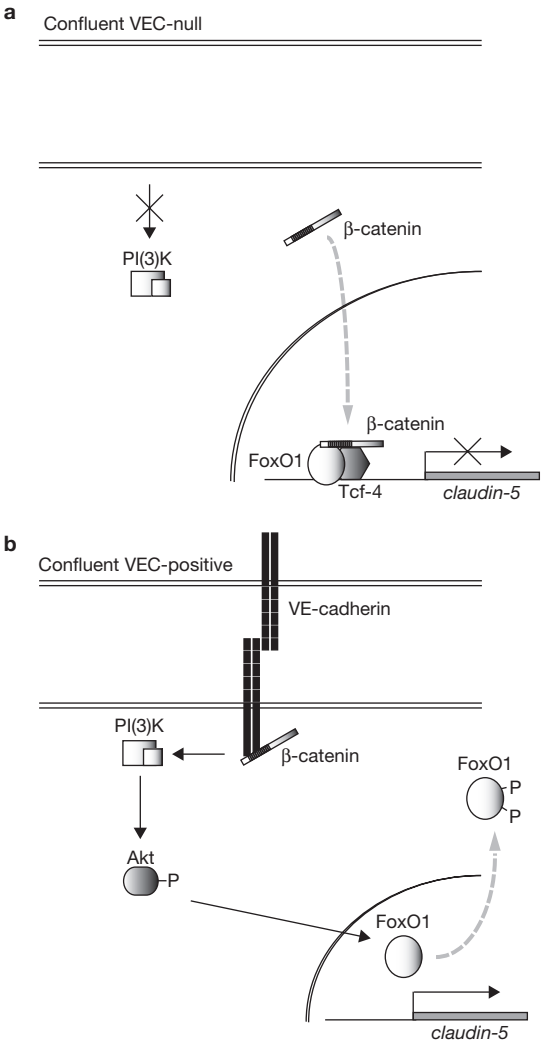

Figure 8 Suggested model for the regulation of claudin-5 expression by VE-cadherin. (**a**) In the absence of VE-cadherin, the FoxO1–β-catenin–Tcf-4 complex binds to the promoter of the *claudin-5* gene and represses its expression. (**b**) On VE-cadherin expression and clustering, FoxO1 is inhibited by Akt-mediated phosphorylation and β-catenin is sequestered at the plasma membrane. This removes the block from the *claudin-5* promoter and allows its upregulation.

β-Catenin and FoxO1 bind the *claudin-5* promoter region at two adjacent sites

A thorough characterization of the *claudin-5* promoter region has not yet been reported. We examined the 6,000 base pairs (bp) upstream of the starting codon of the *claudin-5* coding sequence (CDS) and we identified four pairs of putative FoxO- and Tcf–β-catenin-binding sites localized in three different regions: Region 1, position −2,906/−2,871; Region 2, position −2,317/−2,287; Region 3, position −1,103/−1,008 (Fig. 7a, upper panel).

© 2008 Macmillan Publishers Limited. All rights reserved.

By chromatin immunoprecipitation (ChIP), we checked for interaction of FoxO1 and Tcf–β-catenin with these sequences. In VEC-null cells, FoxO1 (FKHR-TM) could bind Regions 1 and 3, whereas Tcf–β-catenin was present only at Region 1 (Fig. 7a, lower panel). No binding of either FoxO1 or Tcf–β-catenin was found at the level of Region 2. Region 1 therefore seems to be the site at which the interaction between FoxO1 and Tcf–β-catenin takes place.

Quantitative ChIP revealed that FoxO1 and Tcf–β-catenin strongly bind Region 1 of the *claudin-5* promoter only in VEC-null cells and not in VEC-positive cells (Fig. 7b). Thus, low expression of the *claudin-5* gene correlates with high binding of FoxO1 and β-catenin to its 5′ regulatory region.

β-Catenin may increase FoxO1 activity by stabilizing its binding to DNA. To test this possibility, we analysed the strength of FoxO1 binding to Regions 1 and 3 in confluent VEC-null cells. As reported above, both FoxO1 and β-catenin bind Region 1, whereas only FoxO1 binds Region 3 (Fig. 7a). Quantitative ChIP assay showed that FoxO1 binds Region 1 much more strongly than it does Region 3 (Fig. 7c). The binding of β-catenin to region 1 turned out to be dependent on Tcf binding. The overexpression of a dominant-negative form of Tcf-4 (TCF4-DN)[32], comprising the DNA-binding domain but lacking the β-catenin-binding region, abolished β-catenin binding to Region 1 and weakened FoxO1 binding, further confirming the stabilizing role of β-catenin (Fig. 7d).

Taken together, these data are consistent with the idea that β-catenin and FoxO1 act in concert to repress *claudin-5* transcription and suggest that the presence of β-catenin in the complex stabilizes the interaction of FoxO1 with the *claudin-5* promoter (Fig. 8a, b).

DISCUSSION

Here we report, for several cellular and organ systems, that VE-cadherin expression and clustering is required for claudin-5 upregulation. These two junctional proteins are strictly endothelium-specific[14]; a direct and cell-specific relationship between AJ and TJ constituents therefore exists.

The positive relationship between VE-cadherin and claudin-5 may have important functional consequences. Claudins are a multigene family of at least 24 members, each of which has a specific tissue expression pattern[3,33]. They are integral membrane proteins with four-membrane-spanning regions, two extracellular loops and one intracellular loop. These proteins determine the permeability properties of endothelial and epithelial cells by regulating the paracellular flux of water-soluble molecules between adjacent cells. The barrier characteristics vary between cell types, depending on the combination of different claudins. Claudin-5, although not required for vascular development in the embryo, has a non-redundant function in the control of vascular permeability. Newborn *claudin-5*-null mice lack a functional blood–brain barrier[4] and die immediately after birth. In these null pups, TJs in brain microvasculature, although functionally defective, were morphologically normal, suggesting that other junctional components were responsible for the overall junctional architecture.

Consistently, in the present study we found that the lack of VE-cadherin expression and, as a consequence, of claudin-5 expression in cultured cells does not modify the expression or organization of other junctional proteins, but paracellular permeability was significantly increased (Fig. 2c). These data also suggest that modifications of VE-cadherin expression or junctional organization[10,17] may have effects on vascular permeability through modulation of claudin-5 expression and selective alterations in barrier charge and size selectivity.

Previous work[9] and the present study show that VE-cadherin clustering induces PI(3)K activation and Akt phosphorylation. Akt activation triggers different downstream effects and, in particular, inhibits the activity of members of the FoxO family of transcription factors by inducing their phosphorylation[19,21,22].

The results presented here are consistent with the idea that VE-cadherin upregulates claudin-5 indirectly, by releasing the inhibitory effect of FoxO1 through the induction of Akt.

Akt activation is downstream of several growth factor signalling pathways, raising the problem of specificity[34]. The extent and duration of Akt activation may change its downstream effects significantly. Agents important in vascular development activate Akt but it is unclear whether all of them would also inhibit FoxOs and, if so, to which extent and for how long. For instance, the effect of FoxO exclusion from the nucleus promoted by VEGF is transient and reversible, while other factors may present a lasting effect[20]. Considering VE-cadherin, the clustering of this molecule at junctions in confluent ECs induces a persistent and stable increase of claudin-5 which requires a lasting FoxO1 inactivation.

Most importantly, the specificity of the downstream effects of FoxOs is also determined by their association with other transcription factors. For instance, inhibition of nuclear factor-kB (NF-kB) or nuclear factor of activated T cells (NF-AT) attenuates the upregulation of VEGF-induced FoxO dependent genes. FoxOs can interacts with Smads and participate in transforming growth factor-β (TGF-β) signalling[35]. Phosphorylated FoxO1 can interact with Ets-1 (E26 transformation specific sequence-1) and function as coactivator[24,36,37].

Here we report that Tcf–β-catenin form a complex with FoxO1 and cooperate in repressing claudin-5 expression. VE-cadherin expression and clustering inhibits β-catenin nuclear translocation and signalling. This effect may be due to stabilization of VE-cadherin binding to β-catenin in confluent cells. In previous work we found that tyrosine phosphorylation of VE-cadherin and β-catenin is strongly reduced in confluent ECs[38]. Tyrosine phosphorylation of β-catenin[39,40] decreases the affinity of β-catenin binding to cadherin tail and this may explain the differences in nuclear signalling in sparse and confluent cells. In non-transformed cells a considerable amount of β-catenin, once released from junctions, is phosphorylated and ubiquitinated through the action of the adenomatosis polyposis coli (APC)-axin complex[30]. Although this occurs also in VEC-null cells[41], a detectable amount of the Tcf–β-catenin could still be found in the nucleus bound to *claudin-5* promoter even in the absence of GSK3β inhibitors.

Importantly, β-catenin nuclear localization is inversely related to claudin-5 expression suggesting that it may act in concert with FoxO1. This possibility is supported by the observations that FoxO1 and β-catenin form a nuclear complex which binds to *claudin-5* promoter only in the absence of VE-cadherin.

Others[29] found that β-catenin binds to the members of the FoxO subgroup and increases their transcriptional activity both in *C. elegans* and in mammalian cells. However, in these studies Tcf signalling was not involved in the functional interaction. We report here that Tcf is co-precipitated in the β-catenin-FoxO1 complex suggesting that it may participate in claudin-5 repression. An attractive possibility is that Tcf–β-catenin binding acts by stabilizing FoxO1 interaction with the *claudin-5* promoter. This is supported by the fact that FoxO1 can bind to Region 3 of the promoter but this interaction is significantly weaker than that at Region 1, where β-catenin cooperation occurs. Moreover,

© 2008 Macmillan Publishers Limited. All rights reserved.

the inhibition of β-catenin binding to Region 1 by a dominant-negative form of Tcf-4 strongly weakens FoxO1 binding.

In conclusion, an important concept emerging from many studies is that FoxO activity is dependent on context and varies in different types of vessels or with different stimuli[24]. Here we introduce the concept that FoxO1 activity is modulated by the establishment of intercellular junctions. We found that clustering of VE-cadherin may signal by limiting the nuclear localization of the FoxO1–β-catenin complex. Hence, an endothelial-specific AJ protein such as VE-cadherin regulates the expression of another endothelial-specific TJ adhesion protein such as claudin-5, underlining the fine tuning and cellular specificity of junctional organization and permeability control. □

METHODS

Cells and reagents. Cell lines (VEC-null, VEC-positive, e-VE-null, e-VE-positive, β−/−, Δ-βcat, IL2-VEC), antibodies and chemicals used in this study are listed and described in the Supplementary Information, Methods online.

Lentiviral and adenoviral preparations. Two different lentiviral constructs with constitutive Tcf–β-catenin transcriptional activity have been used: LEFΔN-βCTA, (from K. Vleminckx, VIB – University of Gent, Gent, Belgium)[31,42] lacking the armadillo repeats, and ΔN-βcatenin (from C. Brancolini, University of Udine, Udine, Italy), possessing the armadillo repeats. Lentiviral and packaging plasmids were donated by L. Naldini (HSR-TIGET, San Raffaele Telethon Institute for Gene Therapy, Milan, Italy). Lentiviral vectors were produced as described in ref. 43.

Retroviral plasmids for h-claudin-5 and DNAkt1 were donated by P. Adamson (University College London, London, UK) and T. V. Byzova (Joseph J. Jacobs Center for Thrombosis and Vascular Biology, Cleveland, OH, USA)[28], respectively. Retroviruses were produced with the use of standard techniques[44].

The FKHR-TM adenovirus has been described previously[18]. The TCF4-DN adenovirus was donated by S. J. George (Bristol Heart Institute, Bristol, UK)[32]. Infectious viruses were purified and titred with standard techniques. Two consecutive cycles of infection (5 h and overnight) were performed with a multiplicity of infection of 300 in 1 ml of complete culture medium.

Quantitative RT-PCR (qRT–PCR) analysis. Total RNA was isolated by extraction with TRIzol (Invitrogen, Carlsbad, CA, USA) and 1 μg was reverse transcribed with random hexamers (High Capacity cDNA Archive Kit; Applied Biosystems, Foster City, CA, USA) in accordance with the manufacturer's instructions. cDNA (5 ng) was amplified in triplicate in a reaction volume of 15 μl with the TaqMan Gene Expression Assay (Applied Biosystems) and an ABI/Prism 7900 HT thermocycler, using a pre-PCR step of 10 min at 95 °C, followed by 40 cycles of 15 s at 95 °C and 60 s at 60 °C. Preparations of RNA template without reverse transcriptase were used as negative controls. For any sample the expression level, normalized to the housekeeping genes encoding 18S, glyceraldehyde-3-phosphate dehydrogenase (GAPDH) or β_2-microglobulin, was determined with the comparative threshold cycle (C_t) method as described previously[45].

Co-immunoprecipitation. Cells were incubated with 100 μg ml^{-1} dithiobis(succinimidyl)propionate (Pierce, Rockford, IL, USA) for 20 min at 37 °C. Cells were lysed and FoxO1 was immunoprecipitated overnight from nuclear extracts (isolated with a standard nuclear–cytosolic fractionation method[46]). Immunocomplexes were then collected with Gamma-bind beads (Amersham Biosciences, Piscataway, NJ, USA) and immunoprecipitation samples were analysed by standard western blot analysis[38] (see Supplementary Information, Methods online).

Immunofluorescence microscopy. Immunofluorescence microscopy staining was performed with a standard technique described previously[38] (see Supplementary Information, Methods online).

Allantois assay. The allantois assay was performed on allantoises from embryos 8.5 days post coitum (plug date taken as 0.5 days post coitum), essentially as described previously[16]. In brief, allantoises were cultured *ex vivo* for 48 h then fixed with methanol at −20 °C for 5 min and stained with anti-claudin-5 and anti-PECAM (platelet/endothelial cell adhesion molecule) antibodies. Stained allantoises were analysed by scanning confocal microscopy. See details in Supplementary Information, Methods online.

Reporter assays. FoxO activity was measured by the reporter 6×DBE-luc vector, which contains six canonical FoxO-binding sites[47], or by the pSODLUC/pSODLUC-mut reporter system. pSODLUC and pSODLUC-mut plasmids were donated by B. M. T. Burgering (University Medical Center, Utrecht, The Netherlands). The pSODLUC reporter construct contains the FoxO-binding sites of the superoxide dismutase (SOD) promoter, whereas the pSODLUC-mut has point mutations in the first and second FoxO-binding sites and was used as a control[29]. The activation of Tcf–β-catenin-mediated transcription was determined with TOP/FOP constructs (from H. Clevers, Netherlands Institute for Developmental Biology, Utrecht, The Netherlands), respectively named TOP-TK-LUC and FOP-TK-LUC. For details, see Supplementary Information, Methods online.

Oligonucleotide microarray analysis. Synthesis of biotinylated cRNA targets, array hybridization (GeneChips MG_U74Av2 and MG_U74Bv2), staining and scanning were performed in accordance with the Affymetrix (Santa Clara, CA, USA) standard protocols, starting from 15 μg of total RNA. Two copies of the GeneChips were hybridized with each cRNA sample. The MAS5 algorithm was used to determine the expression levels of mRNAs; the absolute analysis was performed with default parameters and a scaling factor of 500. Report files were extracted for each chip, and the performance of labelled target was evaluated on the basis of several values (such as scaling factor, background and noise values, percentage present calls, and average signal value). Gene expression levels were normalized on the median over all samples. Annotation of Probe Sets was performed in accordance with Affymetrix Annotation Tables (release May 31, 2007)[48]. The complete microarray data sets are available from the Gene Expression Omnibus (GSE11674).

Transcription factor binding site analysis. To identify FoxO1 and Tcf–β-catenin consensus sequences on the putative *claudin-5* promoter region we used the program MatInspector[49], which identifies transcription-factor-binding sites in nucleotide sequences using a large library of weight matrices. We analysed the 6,000 bp upstream of the *claudin-5* CDS and obtained a prediction of a potential combination of transcription-factor-binding sites with reasonable accuracy. The sequences of the transcription-factor-binding sites considered in the analysis were [AG][GA][TG][AC]AACAA[AC] for FoxO1 binding and [TAG][GT][AG][CT][AT]x(2)CAAAG[GCT][GAC][AC][GCA] for Tcf–β-catenin binding.

Chromatin immunoprecipitation. ChIP assays were performed as described previously[50]. In brief, cells were starved overnight and crosslinked with 1% paraformaldehyde (PAF) for 10 min at 18–25 °C. PAF was then inactivated by the addition of 125 mM glycine. Cells were then washed and resuspended in lysis buffer. Samples were sonicated with a BIORUPTOR200 with the following conditions: H power, 30 s ON–60 s OFF for 20 min. Chromatin extracts containing 200 μg of DNA fragments with an average size of 500 bp were immunoprecipitated with 5 μg of antibody. DNA was recovered and amplified by standard PCR or qRT-PCR techniques with the use of oligonucleotides flanking the assayed promoter regions.

Primers used in this experiment were as follows: 5′-CTGCTGAACTTGGGGAAGAC-3′ and 5′-AAGGGAGTGAGGGAAGGAAA-3′ (Region 1); 5′-GCTGGGTTTTGCCTTCCTAT-3′ and 5′-CACACAGCACAGGCCACTTA-3′ (Region 2); 5′-ACCCCCAAACAGAACAACAA-3′ and 5′-GTGAACACTCCTCCCTGCTC-3′ (Region 3).

Moreover, claudin-5 primers for the *claudin-5* coding sequence (NM_013805) were used as a negative control to exclude non-specific precipitated DNA: 5′-GGCACTCTTTGTTACCTTGACC-3′ and 5′-CAGCTCGTACTTCTGTGACACC-3′. For qualitative PCR analyses we used the following PCR conditions: 94 °C for 2 min; (94 °C for 30 s; 54 °C (Regions 1, 2 and 3) and 64 °C (*claudin-5* CDS) for 30 s; 72 °C for 1 min) for 33 cycles; 72 °C for 7 min.

For qRT-PCR analyses DNA was diluted with specific primers (10 mM each) to a final volume of 25 μl in SYBR Green Reaction Mix (Perking Elmer, Waltham, MA, USA).

RNA interference. Stealth RNAi Duplexes and the corresponding Low or Medium GC Stealth RNAi Control Duplexes (Invitrogen) were used to knockdown *claudin-5*, *Akt1* and *FoxO1*. The *claudin-5* target sequences used were as follows: 5′-GCAGUGCAAGGUGUAUGAAUCUGUG-3′ (siRNA no. 1) and

© 2008 Macmillan Publishers Limited. All rights reserved.

5′-CACAUGCAGUGCAAGGUGUAUGAAU-3′ (siRNA no. 2). The Akt1 target sequence was 5′-CAACAUCGUGUGGCAGGAUGUGUAU-3′. The FoxO1 target sequence was 5′-GAGAAUGAAGGAACUGGAAAGAGUU-3′. Transfection was performed with LipofectAMINE 2000 (Invitrogen) in accordance with the manufacturer's instructions.

Paracellular tracer flux analysis. VEC-positive cells were seeded on 6.5-mm diameter Transwell Permeable Supports (Corning, Corning, NY, USA), cultured in complete culture medium and assayed for permeability to fluorescein isothiocyanate (FITC)-dextran (38 kDa) (Sigma, St Louis, MO, USA). See details of the procedure in the Supplementary Information, Methods online.

Statistical analysis. Student's two-tailed non-paired *t*-test or analysis of variance and a Dunnett test for multiple comparisons were used to determine statistical significance. The significance level was set at $P < 0.05$.

Note: Supplementary Information is available on the Nature Cell Biology website.

ACKNOWLEDGEMENTS

We thank Barbara Felice for help in the transcription-factor-binding-site analysis. This work was supported by the Associazione Italiana per la Ricerca sul Cancro, Association for International Cancer Research, the European Community (Integrated Project Contract No LSHG-CT-2004-503573; NoE MAIN 502935; NoE EVGN 503254; EUSTROKE and OPTISTEM Networks), Istituto Superiore di Sanita', Italian Ministry of Health, MIUR (COFIN prot: 2006058482_002), Fondation Leducq Transatlantic Network of Excellence. C.G. is supported by an AIRC-SISAL fellowship.

AUTHOR CONTRIBUTIONS

E.D. and A.T. planned the experimental design. E.D., A.T. and C.G. analysed data and conducted the scientific writing. A.T. and C.G. performed the experimental work. A.C. analysed the Affymetrix data. F.O. and F.B. provided molecular biology support. V.P. performed the TOP/FOP assay. M.P., C.D. and S.D. provided scientific input and reagents.

COMPETING FINANCIAL INTERESTS

The authors declare no competing financial interests.

Published online at http://www.nature.com/naturecellbiology/
Reprints and permissions information is available online at http://npg.nature.com/reprintsandpermissions/

1. Dejana, E. Endothelial cell–cell junctions: happy together. *Nature Rev. Mol. Cell Biol.* **5,** 261–270 (2004).
2. Gumbiner, B. M. Regulation of cadherin-mediated adhesion in morphogenesis. *Nature Rev. Mol. Cell Biol.* **6,** 622–634 (2005).
3. Furuse, M. & Tsukita, S. Claudins in occluding junctions of humans and flies. *Trends Cell Biol.* **16,** 181–188 (2006).
4. Nitta, T. *et al.* Size-selective loosening of the blood–brain barrier in claudin-5-deficient mice. *J. Cell Biol.* **161,** 653–660 (2003).
5. Ikenouchi, J., Umeda, K., Tsukita, S., Furuse, M. & Tsukita, S. Requirement of ZO-1 for the formation of belt-like adherens junctions during epithelial cell polarization. *J. Cell Biol.* **176,** 779–786 (2007).
6. Miyoshi, J. & Takai, Y. Molecular perspective on tight-junction assembly and epithelial polarity. *Adv. Drug Deliv. Rev.* **57,** 815–855 (2005).
7. Ohsugi, M., Larue, L., Schwarz, H. & Kemler, R. Cell-junctional and cytoskeletal organization in mouse blastocysts lacking E-cadherin. *Dev. Biol.* **185,** 261–271 (1997).
8. Behrens, J., Birchmeier, W., Goodman, S. L. & Imhof, B. A. Dissociation of Madin–Darby canine kidney epithelial cells by the monoclonal antibody anti-arc-1: mechanistic aspects and identification of the antigen as a component related to uvomorulin. *J. Cell Biol.* **101,** 1307–1315 (1985).
9. Carmeliet, P. *et al.* Targeted deficiency or cytosolic truncation of the VE-cadherin gene in mice impairs VEGF-mediated endothelial survival and angiogenesis. *Cell* **98,** 147–157 (1999).
10. Corada, M. *et al.* Vascular endothelial-cadherin is an important determinant of microvascular integrity *in vivo*. *Proc. Natl Acad. Sci. USA* **96,** 9815–9820 (1999).
11. Liebner, S., Cavallaro, U. & Dejana, E. The multiple languages of endothelial cell-to-cell communication. *Arterioscler. Thromb. Vasc. Biol.* **26,** 1431–1438 (2006).
12. Wheelock, M. J. & Johnson, K. R. Cadherin-mediated cellular signaling. *Curr. Opin. Cell Biol.* **15,** 509–514 (2003).
13. Lampugnani, M. G. *et al.* Contact inhibition of VEGF-induced proliferation requires vascular endothelial cadherin, β-catenin, and the phosphatase DEP-1/CD148. *J. Cell Biol.* **161,** 793–804 (2003).
14. Xiao, K. *et al.* Mechanisms of VE-cadherin processing and degradation in microvascular endothelial cells. *J. Biol. Chem.* **278,** 19199–19208 (2003).
15. Lampugnani, M. G. *et al.* VE-cadherin regulates endothelial actin activating Rac and increasing membrane association of Tiam. *Mol. Biol. Cell* **13,** 1175–1189 (2002).
16. Crosby, C. V. *et al.* VE-cadherin is not required for the formation of nascent blood vessels but acts to prevent their disassembly. *Blood* **105,** 2771–2776 (2005).
17. Gavard, J. & Gutkind, J. S. VEGF controls endothelial-cell permeability by promoting the β-arrestin-dependent endocytosis of VE-cadherin. *Nature Cell Biol.* **8,** 1223–1234 (2006).
18. Daly, C. *et al.* Angiopoietin-1 modulates endothelial cell function and gene expression via the transcription factor FKHR (FOXO1). *Genes Dev.* **18,** 1060–1071 (2004).
19. Burgering, B. M. & Kops, G. J. Cell cycle and death control: long live Forkheads. *Trends Biochem. Sci.* **27,** 352–360 (2002).
20. Potente, M. *et al.* Involvement of Foxo transcription factors in angiogenesis and postnatal neovascularization. *J. Clin. Invest* **115,** 2382–2392 (2005).
21. Brunet, A. *et al.* Akt promotes cell survival by phosphorylating and inhibiting a Forkhead transcription factor. *Cell* **96,** 857–868 (1999).
22. Zhang, X. *et al.* Phosphorylation of serine 256 suppresses transactivation by FKHR (FOXO1) by multiple mechanisms. Direct and indirect effects on nuclear/cytoplasmic shuttling and DNA binding. *J. Biol. Chem.* **277,** 45276–45284 (2002).
23. Gilley, J., Coffer, P. J. & Ham, J. FOXO transcription factors directly activate *bim* gene expression and promote apoptosis in sympathetic neurons. *J. Cell Biol.* **162,** 613–622 (2003).
24. Paik, J. H. *et al.* FoxOs are lineage-restricted redundant tumor suppressors and regulate endothelial cell homeostasis. *Cell* **128,** 309–323 (2007).
25. Lee, S. *et al.* Autocrine VEGF signaling is required for vascular homeostasis. *Cell* **130,** 691–703 (2007).
26. Sini, P. *et al.* Inhibition of multiple vascular endothelial growth factor receptors (VEGFR) blocks lymph node metastases but inhibition of VEGFR-2 is sufficient to sensitize tumor cells to platinum-based chemotherapeutics. *Cancer Res.* **68,** 1581–1592 (2008).
27. Faivre, S., Demetri, G., Sargent, W. & Raymond, E. Molecular basis for sunitinib efficacy and future clinical development. *Nature Rev. Drug Discov.* **6,** 734–745 (2007).
28. Chen, J. *et al.* Akt1 regulates pathological angiogenesis, vascular maturation and permeability *in vivo*. *Nature Med.* **11,** 1188–1196 (2005).
29. Essers, M. A. *et al.* Functional interaction between β-catenin and FOXO in oxidative stress signaling. *Science* **308,** 1181–1184 (2005).
30. Clevers, H. Wnt/β-catenin signaling in development and disease. *Cell* **127,** 469–480 (2006).
31. Vleminckx, K., Kemler, R. & Hecht, A. The C-terminal transactivation domain of β-catenin is necessary and sufficient for signaling by the LEF-1/β-catenin complex in *Xenopus laevis*. *Mech. Dev.* **81,** 65–74 (1999).
32. Quasnichka, H. *et al.* Regulation of smooth muscle cell proliferation by β-catenin/T-cell factor signaling involves modulation of cyclin D1 and p21 expression. *Circ. Res.* **99,** 1329–1337 (2006).
33. Van Itallie, C. M. & Anderson, J. M. Claudins and epithelial paracellular transport. *Annu. Rev. Physiol* **68,** 403–429 (2006).
34. Dimmeler, S. & Zeiher, A. M. Akt takes center stage in angiogenesis signaling. *Circ. Res.* **86,** 4–5 (2000).
35. Seoane, J., Le, H. V., Shen, L., Anderson, S. A. & Massagué, J. Integration of Smad and forkhead pathways in the control of neuroepithelial and glioblastoma cell proliferation. *Cell* **117,** 211–223 (2004).
36. Asada, S. *et al.* Mitogen-activated protein kinases, Erk and p38, phosphorylate and regulate Foxo1. *Cell Signal.* **19,** 519–527 (2007).
37. Dejana, E., Taddei, A. & Randi, A. M. Foxs and Ets in the transcriptional regulation of endothelial cell differentiation and angiogenesis. *Biochim. Biophys. Acta* **1775,** 298–312 (2007).
38. Lampugnani, M. G. *et al.* Cell confluence regulates tyrosine phosphorylation of adherens junction components in endothelial cells. *J. Cell Sci.* **110,** 2065–2077 (1997).
39. Roura, S., Miravet, S., Piedra, J., Garcia de, H. A. & Dunach, M. Regulation of E-cadherin/Catenin association by tyrosine phosphorylation. *J. Biol. Chem.* **274,** 36734–36740 (1999).
40. Huber, A. H. & Weis, W. I. The structure of the β-catenin/E-cadherin complex and the molecular basis of diverse ligand recognition by β-catenin. *Cell* **105,** 391–402 (2001).
41. Zanetta, L. *et al.* Downregulation of vascular endothelial-cadherin expression is associated with an increase in vascular tumor growth and hemorrhagic complications. *Thromb. Haemost.* **93,** 1041–1046 (2005).
42. Cattelino, A. *et al.* The conditional inactivation of the β-catenin gene in endothelial cells causes a defective vascular pattern and increased vascular fragility. *J. Cell Biol.* **162,** 1111–1122 (2003).
43. Dull, T. *et al.* A third-generation lentivirus vector with a conditional packaging system. *J. Virol.* **72,** 8463–8471 (1998).
44. Pear, W. S., Nolan, G. P., Scott, M. L. & Baltimore, D. Production of high-titer helper-free retroviruses by transient transfection. *Proc. Natl Acad. Sci. USA* **90,** 8392–8396 (1993).
45. Spagnuolo, R. *et al.* Gas1 is induced by VE-cadherin and vascular endothelial growth factor and inhibits endothelial cell apoptosis. *Blood* **103,** 3005–3012 (2004).
46. Grueneberg, D. A. *et al.* A functional screen in human cells identifies UBF2 as an RNA polymerase II transcription factor that enhances the β-catenin signaling pathway. *Mol. Cell Biol.* **23,** 3936–3950 (2003).
47. Furuyama, T., Nakazawa, T., Nakano, I. & Mori, N. Identification of the differential distribution patterns of mRNAs and consensus binding sequences for mouse DAF-16 homologues. *Biochem. J.* **349,** 629–634 (2000).
48. Vecchi, M. *et al.* Gene expression analysis of early and advanced gastric cancers. *Oncogene* **26,** 4284–4294 (2007).
49. Cartharius, K. *et al.* MatInspector and beyond: promoter analysis based on transcription factor binding sites. *Bioinformatics* **21,** 2933–2942 (2005).
50. Nakae, J. *et al.* The forkhead transcription factor Foxo1 regulates adipocyte differentiation. *Dev. Cell* **4,** 119–129 (2003).

© 2008 Macmillan Publishers Limited. All rights reserved.

nature cell biology

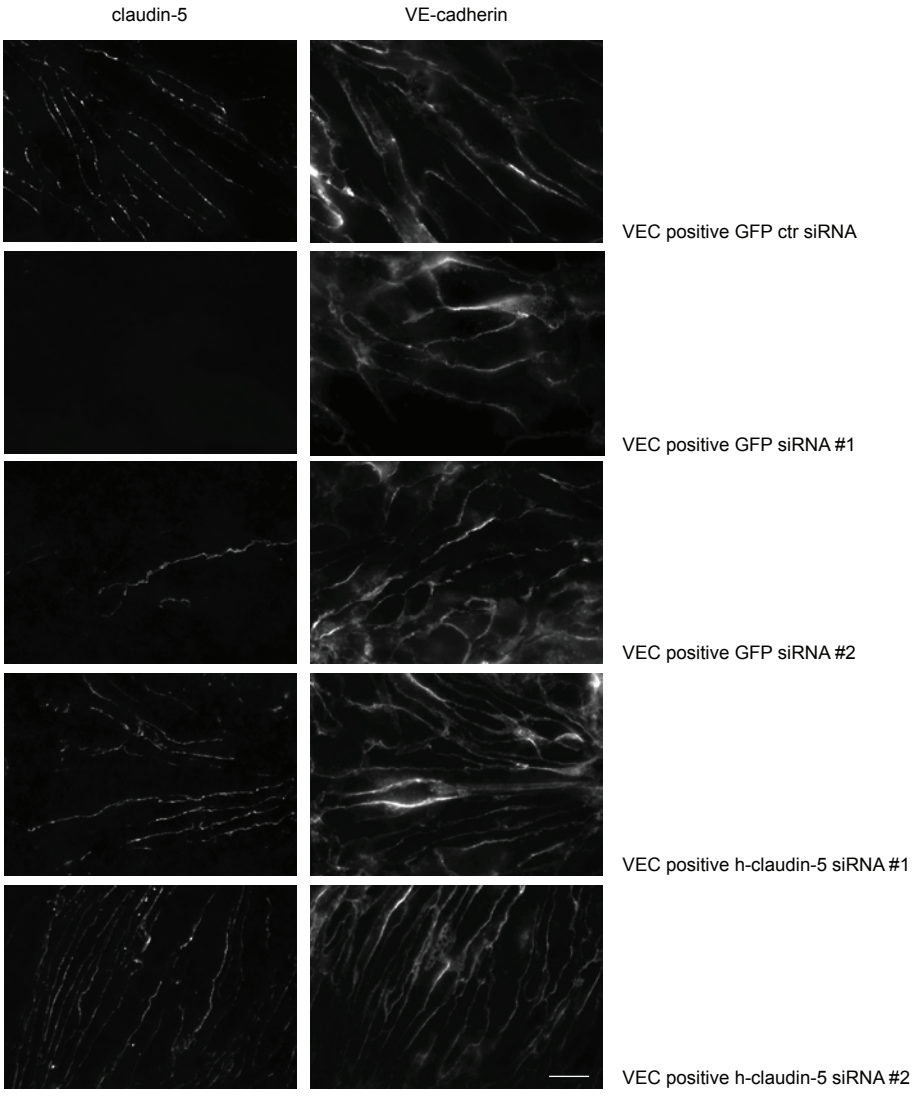

Figure S1 Claudin-5 knock-down does not alter VE-cadherin organization at cell-cell junctions. Immunofluorescence analysis of VEC positive GFP and VEC positive h-claudin-5 cells transfected with ctr siRNA or anti-claudin-5 siRNA #1 and #2. Cells were double stained with anti-claudin-5 (left panels) and anti-VE-cadherin (right panels) Abs. Immunofluorescence was performed directly on Transwell Permeable Supports membranes of the pracellular tracer flux assay of Fig. 2c. No significant alteration of VE-cadherin junctional distribution was observed upon claudin-5 knock-down. Scale bar = 10 μm.

© 2008 Macmillan Publishers Limited. All rights reserved.

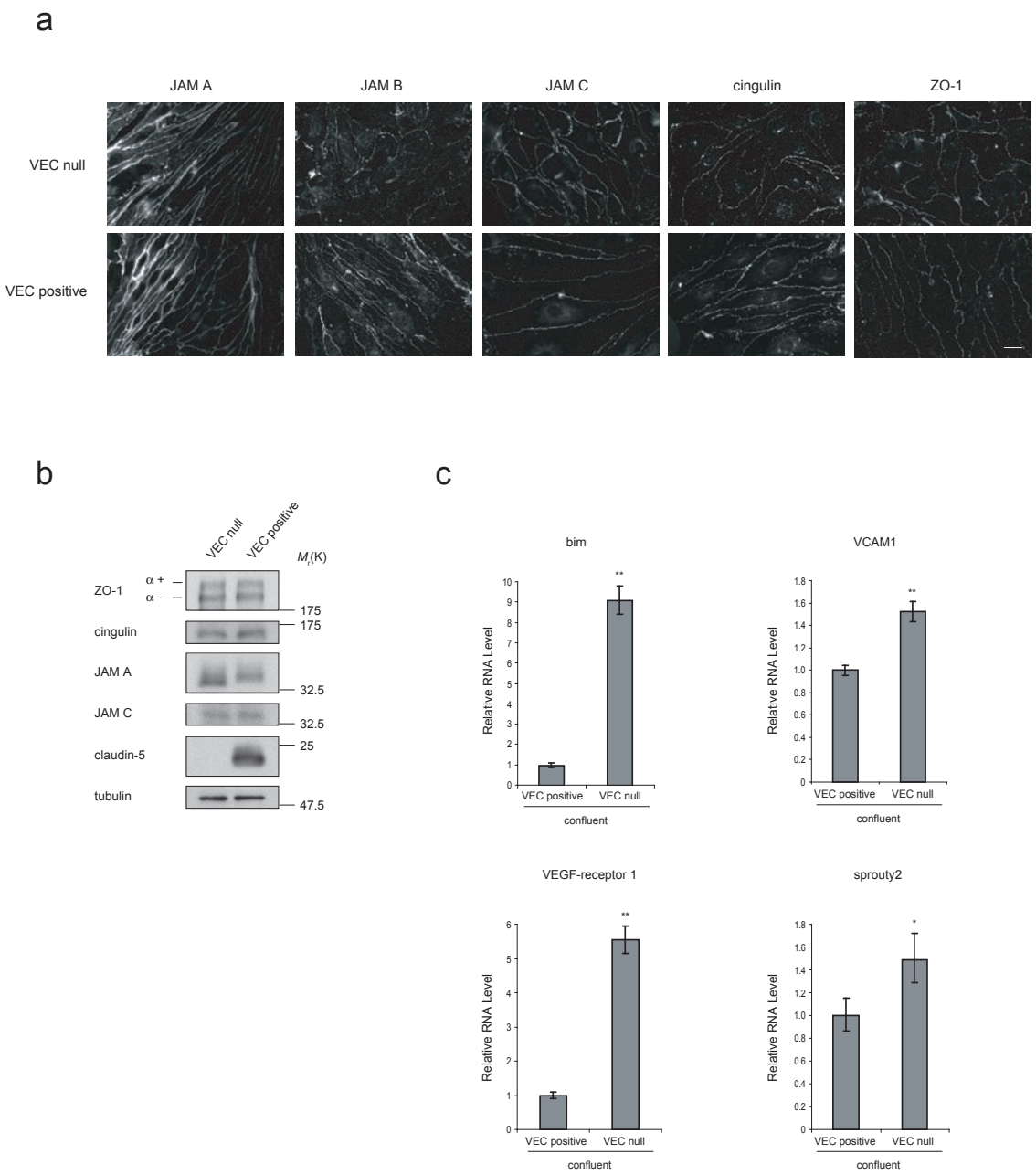

Figure S2 (a) and (b) Effect of VE-cadherin on TJ molecules' expression and organization; **(c)** VE-cadherin negative regulation of FoxO1 target genes. (**a**) Immunofluorescence microscopy of confluent VEC positive and VEC null cells stained with anti-JAM A, -JAM B, -JAM C , -cingulin and -ZO-1 Abs. No major differences of junctional proteins' distribution were observed in the presence or absence of VE-cadherin. Scale bar = 10 μm. (**b**) Western blot analysis of ZO-1, cingulin, JAM A, JAM C and claudin-5 expression in extracts of VEC null and positive cells in the confluent condition. No major differences of junctional proteins' expression, other than claudin-5, were observed in the presence or absence of VE-cadherin. Tubulin is shown as loading control.The experiments shown in (a) and (b) were performed twice with comparable results. (**c**) Analysis of FoxO1 target gene expression. Quantitative RT-PCR of bim, VCAM1, VEGF-receptor 1 and sprouty2 performed on confluent VEC null and VEC positive cells. All these target genes are up-regulated when FoxO1 activity is increased such as in VEC null cells. The levels of mRNA are normalized to 18S, columns are means ± s.e.m. of triplicates from a representative experiment (n=3; *t*-test: $*P < 0.05$; $**P < 0.01$).

© 2008 Macmillan Publishers Limited. All rights reserved.

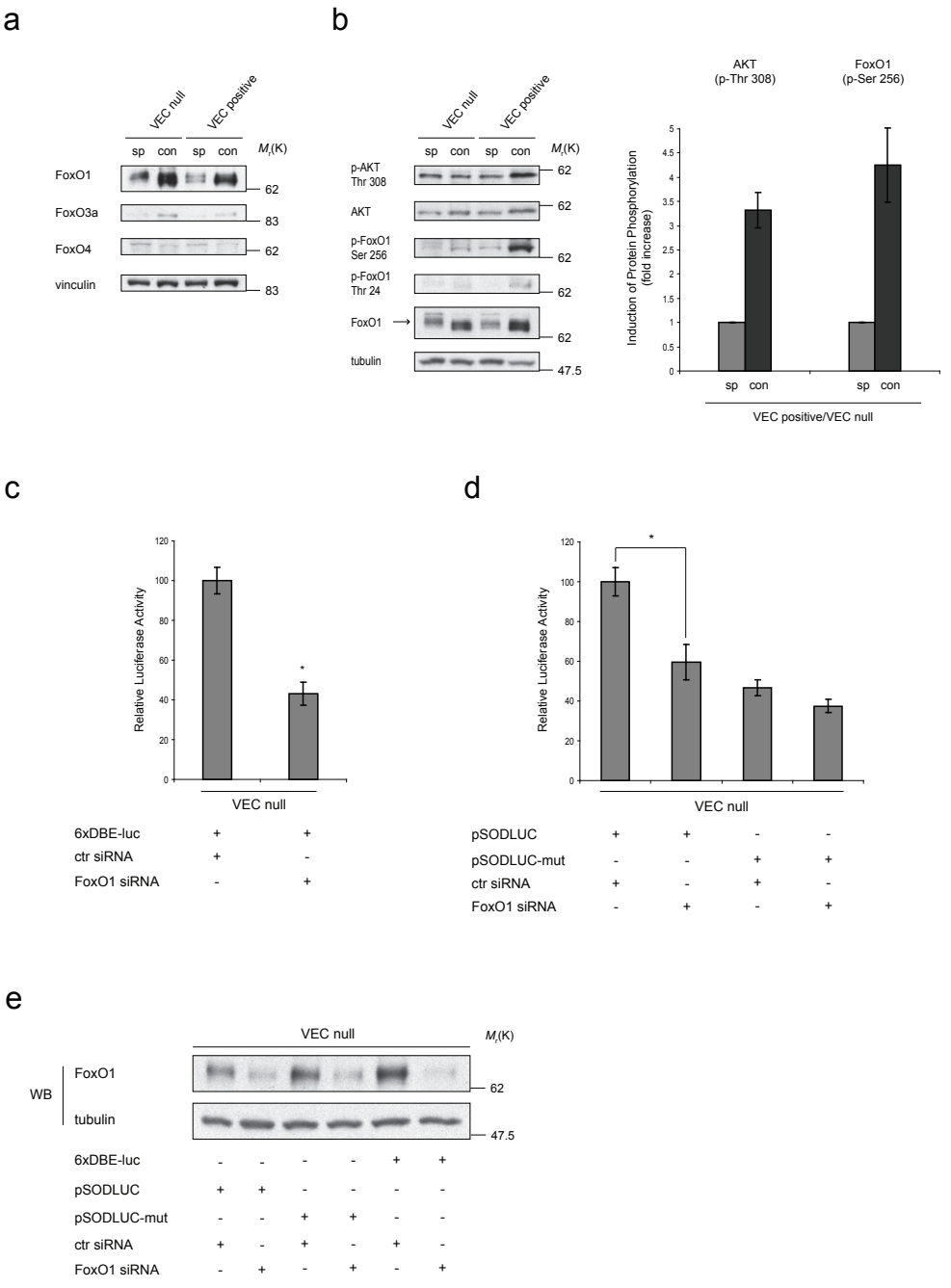

Figure S3 (a) and (b) AKT and FoxO1 phosphorylation in sparse cells; **(c), (d) and (e)** sensitivity of 6xDBE-luc and pSODLUC reporters to endogenous FoxO1 levels. (**a**) Western blot analysis of FoxO1, FoxO3a and FoxO4 in total cell lysates of sparse and confluent VEC null and positive cells. FoxO1 expression level appeared much higher than FoxO3a and FoxO4 levels both in sparse and confluent cells. (**b**) AKT and FoxO1 phosphorylation (p-Akt Thr 308 and p-FoxO1 Ser 256 and Thr 24 respectively) in sparse and confluent VEC null and positive cells. Cells were grown to confluence then starved for 24 h. Total cell lysates were analysed in Western blot for phosphorylated and total AKT and FoxO1 expression using specific Abs. Phosphorylated AKT and FoxO1 signals (Thr 308 and Ser 256 respectively) were normalized to the corresponding total protein amount. For sake of clarity, the normalized phosphorylation levels of VEC positive cells have been divided by those of VEC null, both for the sparse and confluent conditions, to obtain an index of the induction of protein phosphorylation mediated by VE-cadherin expression. VE-cadherin expression induced a much higher AKT and FoxO1 phosphorylation in confluent than in sparse cells. Columns are means ± s.e.m. of three independent experiments performed. (**c**) FoxO transcriptional activity. VEC null cells were simultaneously transfected with the 6xDBE-luc reporter and either ctr or anti-FoxO1 siRNA. FoxO1 knock-down determined a strong reduction of the luciferase reporter activity. (**d**) FoxO transcriptional activity. VEC null cells were simultaneously transfected with either pSODLUC or control pSODLUC-mut reporters, together with ctr or anti-FoxO1 siRNA. FoxO1 knock-down induced the reduction of pSODLUC reporter signal, while the activity pSODLUC-mut was not significantly affected. In (c) and (d) data are means ± s.e.m. of six replicates from a representative experiment (n=3; *t*-test: $*P < 0.01$). (**e**) Western blot analysis of FoxO1 in confluent VEC null cells transfected with the indicated constructs and siRNAs. Tubulin is shown as loading control.

© 2008 Macmillan Publishers Limited. All rights reserved.

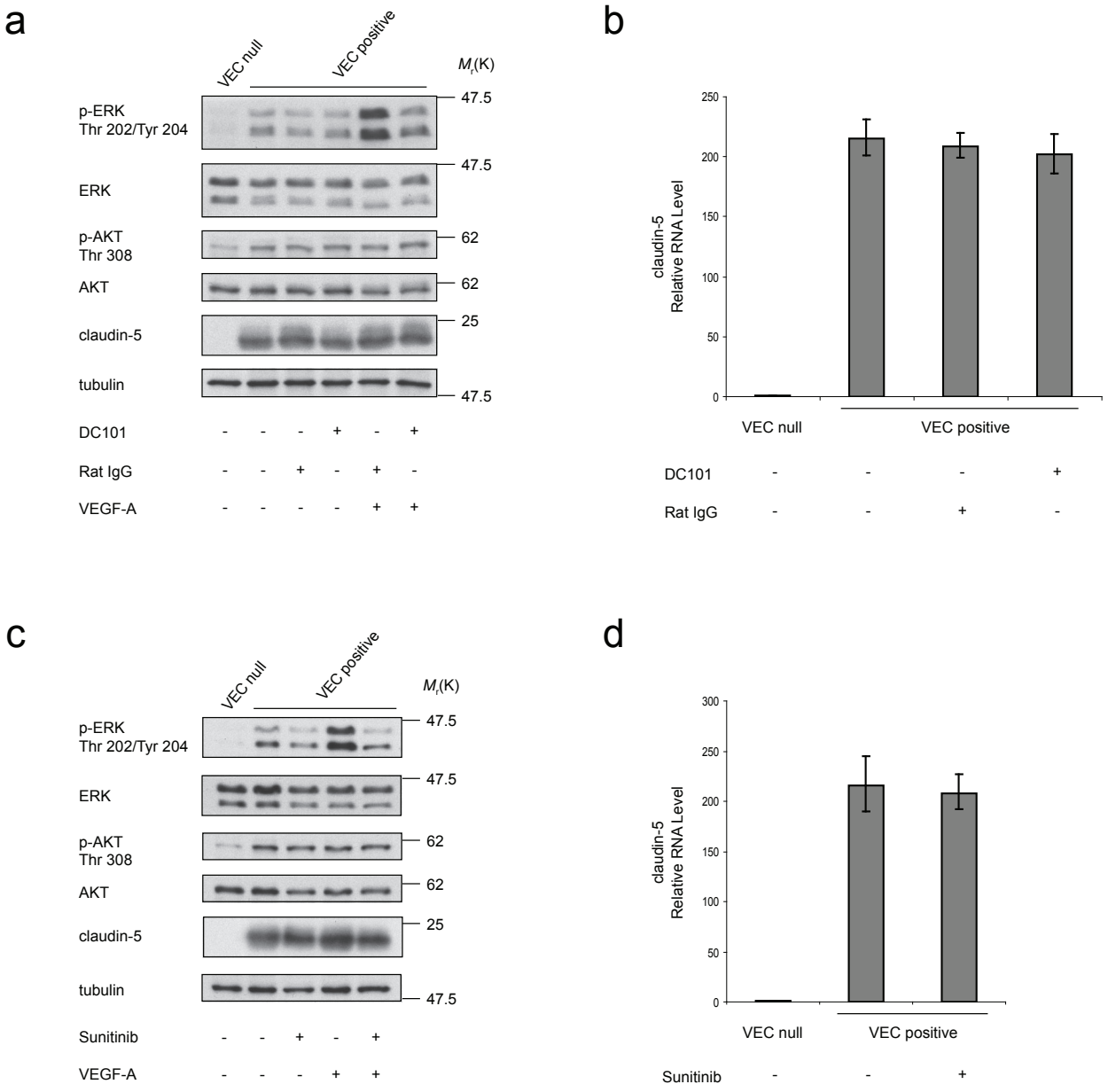

Figure S4 AKT activation and claudin-5 up-regulation by VE-cadherin clustering are independent of VEGF signalling. (**a**) Western blot analysis of AKT and ERK phosphorylation (p-Akt Thr 308 and p-ERK Thr 202 and Tyr 204 respectively) and claudin-5 expression. Cells were grown to 90% of confluence then starved for 72 h in the presence of DC101 Ab (15 µg/ml) or Rat IgG as control. The inhibition of exogenous VEGF-A-induced (80 ng/ml, 10 min) ERK phosphorylation was assayed as control for DC101 Ab efficiency. No inhibition of VE-cadherin-induced AKT phosphorylation and claudin-5 up-regulation was observed upon DC101 Ab treatment. (**b**) Quantitative RT-PCR analysis of claudin-5 expression in confluent VEC null cells and VEC positive cells treated with DC101 Ab or Rat IgG. (**c**) Western blot analysis of AKT and ERK phosphorylation (p-Akt Thr 308 and p-ERK Thr 202 and Tyr 204 respectively) and claudin-5 expression. Cells were cultured as described in (a) then starved for 72 h in the presence of Sunitinib (0.5 µM). The inhibition of exogenous VEGF-A-induced (80 ng/ml, 10 min) ERK phosphorylation was assayed as control for Sunitinib efficiency. Sunitinib treatment did not inhibit VE-cadherin-induced AKT phosphorylation and claudin-5 up-regulation. In (a) and (c) tubulin is shown as loading control (n=3). (**d**) Quantitative RT-PCR analysis of claudin-5 expression in confluent VEC null cells and VEC positive cells treated with Sunitinib. In (b) and (d) the levels of mRNA are normalized to GAPDH, columns are means ± s.e.m. of triplicates from a representative experiment (n=3).

© 2008 Macmillan Publishers Limited. All rights reserved.

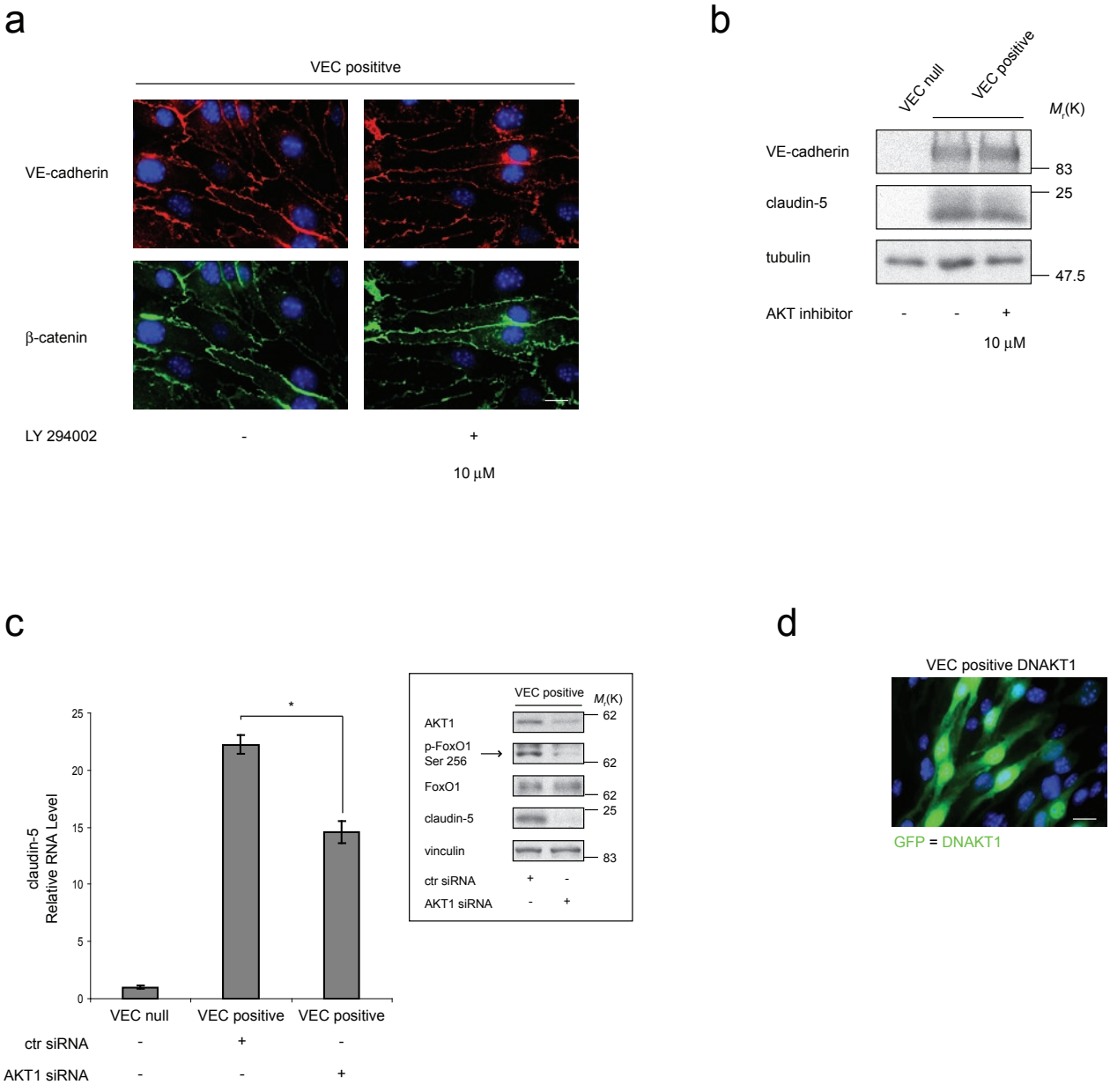

Figure S5 The AKT pathway controls claudin-5 expression. (**a**) Immunofluorescence analysis of VEC positive cells in the presence of the PI3K inhibitor LY 294002 (10 μM). Cells were cultured as described in Fig. 4a and double stained with anti-VE-cadherin (red, upper panels) and anti-β-catenin (green, lower panels) Abs. LY 294002 treatment did not alter VE-cadherin and β-catenin junctional localization. Scale bar = 10 μm. (**b**) Western blot analysis of VE-cadherin and claudin-5 expression in confluent VEC null cells and VEC positive cells upon treatment with the AKT inhibitor (see Fig. 4b). VE-cadherin expression was not altered by AKT inhibition. As expected, due to the short period of AKT inhibitor treatment (8 h), no reduction of claudin-5 protein amount could be detected. Tubulin is shown as loading control. The experiment was performed three times with comparable results. (**c**) Quantitative RT-PCR analysis of claudin-5 expression upon AKT1 knock-down. Inner panel: Western blot analysis of AKT1, p-FoxO1 Ser 256, total FoxO1 and claudin-5 in confluent VEC positive cells transfected with ctr or anti-AKT1 siRNA. Vinculin is shown as loading control. The levels of mRNA are normalized to β2-microglobulin, columns are means ± s.e.m. of triplicates from a representative experiment (n=3; *t*-test: $*P < 0.01$). (**d**) Immunofluorescence analysis of VEC positive cells infected with DNAKT1 retroviral vector. GFP signal corresponds to DNAKT1 expression . The percentage of cells expressing DNAKT1 was assayed by counting GFP-positive cells and was around 50%. Scale bar = 10 μm.

© 2008 Macmillan Publishers Limited. All rights reserved.

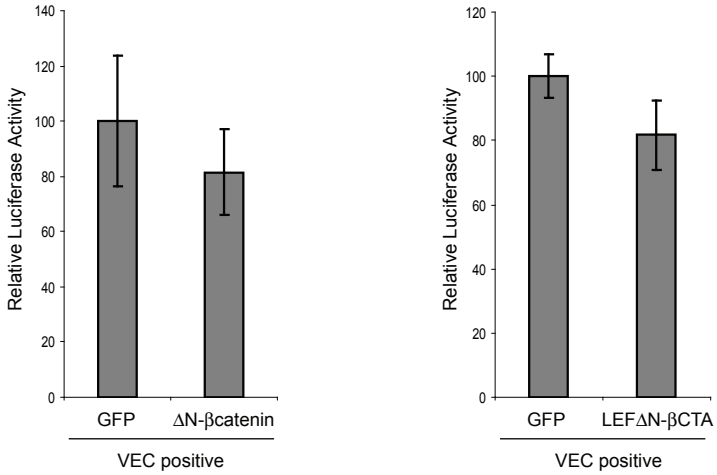

Figure S6 FoxO transcriptional activity analysis upon expression of β-catenin mutants. FoxO transcriptional activity. The activity was measured using the luciferase reporter 6xDBE-luc vector, containing 6 FoxO binding sites but no sites for Tcf-β-catenin binding. No change in FoxO transcriptional activity was detected upon expression of ΔN-βcatenin or LEFΔN-βCTA mutants in confluent VEC positive cells. Data are represented as means ± s.e.m. of six replicates from a representative experiment out of three performed.

© 2008 Macmillan Publishers Limited. All rights reserved.

Figure 1c

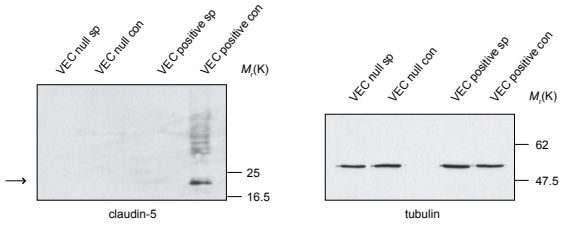

Figure 3b

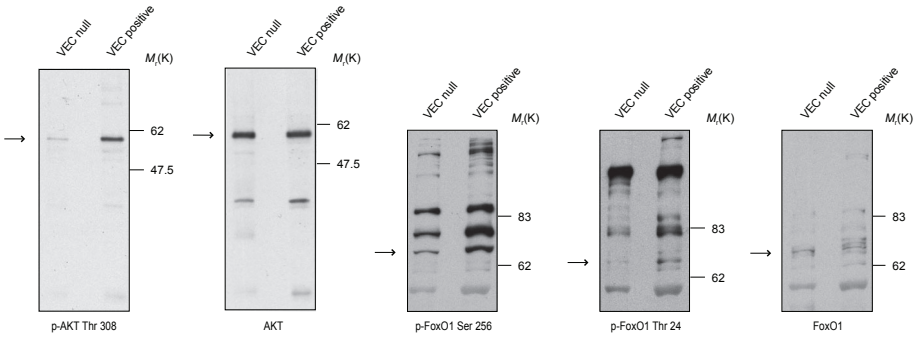

Figure 3c

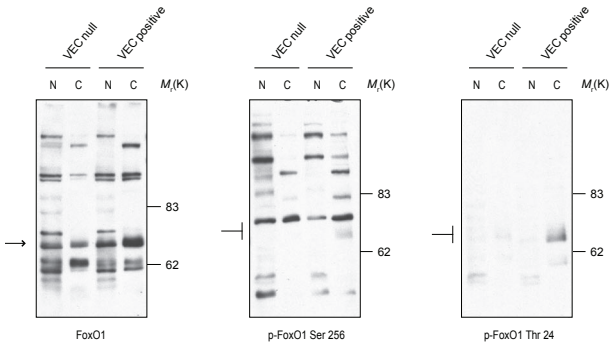

Figure 5a

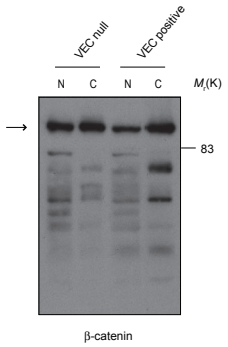

Figure 5d

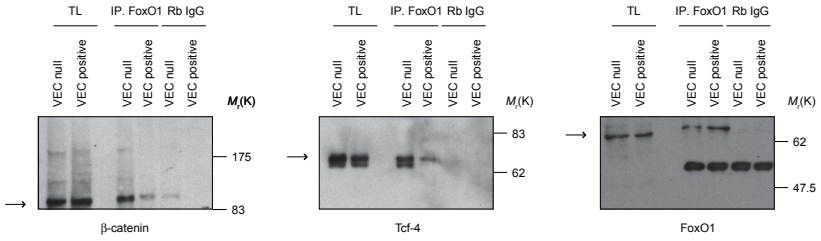

Figure 6f

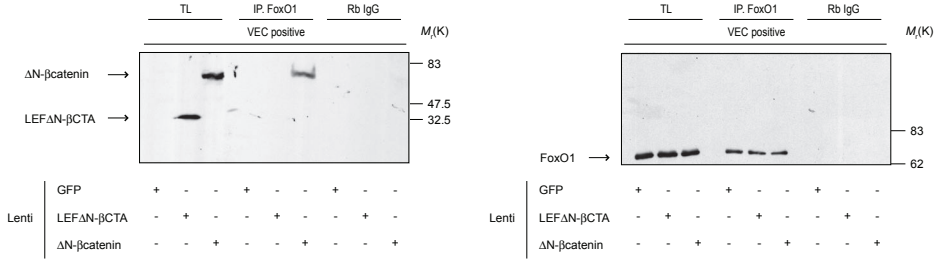

Figure S7 Full scans of key Western bots shown in Fig. 1, 3, 5 and 6.

© 2008 Macmillan Publishers Limited. All rights reserved.

SUPPLEMENTARY INFORMATION

METHODS

Cell culture. Cell lines used in this study were:

ECs derived from murine embryonic stem cells with homozygous null mutation of the VE-cadherin gene (VEC null)[51]. The wild type form of VE-cadherin was introduced in these cells (VEC positive) as described in detail by Lampugnani et al.[13].

β-Catenin-null cells (β-/-), homozygously null mutated in the β-catenin gene[52], isolated from 9.5 dpc embryos[51].

Δ-βCat cells, ECs expressing a truncated mutant of VE-cadherin (lacking aa 703-784 of human VE-cadherin[53], which correspond to β-catenin binding region)[13].

IL2-VEC cells, ECs expressing a mutated version of VE-cadherin made up of VE-cadherin cytoplasmic domain (aa 621-784) fused to the extracellular and transmembrane domains of interleukin-2 receptor α-chain (from Andrew Kowalczyk, Emory University, Atlanta, GA)[14,15].

ECs isolated from 9 dpc mouse embryos homozygous for a null mutation in the VE-cadherin gene (e-VE null)[54], and the same cells transduced with the wild type VE-cadherin sequence (e-VE positive).

Adult ECs isolated from lung of wild type adult mice as described[51, 55].

For all ECs of murine origin, culture medium was DMEM with 20% FCS, glutamine (2 mM), penicillin/streptomycin (100 units/L), sodium pyruvate (1mM), heparin (100 μg/ml, from porcine intestinal mucosa; Sigma), and endothelial cell growth supplement (ECGS) (5 μg/ml, made from calf brain) (complete culture medium).

Starving medium was MCDB 131 (GIBCO, Invitrogen) with 1% bovine serum albumin (BSA) (EuroClone, Milan, Italy), glutamine (2 mM), penicillin/streptomycin (100 units/L) and sodium pyruvate (1mM).

© 2008 Macmillan Publishers Limited. All rights reserved.

Epithelial AD-HEK293 cell line (human embryonic kidney, American Type Culture Collection, Manassas, VA), used for adenoviral production, was grown in DMEM medium (Cambrex Bioscience, East Rutherford, NJ) supplemented with 10% FBS N/A (HyClone), glutamine (2 mM), penicillin/streptomycin (100 units/L), and sodium pyruvate (1 mM).
All cells were cultured at 37°C in a humidified atmosphere of 5% CO_2/air.

Allantois assay. Allantoises from 8.5 dpc embryos (0.5 dpc, plug date) were excised, washed in cold PBS and then placed into Nunc 4-chambered culture slides (Nalgene Nunc International, Rochester, NY) containing 0.4 ml of DMEM (GIBCO, Invitrogen) supplemented with 10% fetal calf serum (FCS) (HyClone, Logan, Utah), glutamine (2 mM; Sigma), penicillin/streptomycin (100 units/L; Sigma), sodium pyruvate (1mM; Sigma). Explants were cultured at 37°C in a 5% CO_2 incubator for 48 h and then fixed with -20°C methanol for 5 min.
The explants were blocked in 2.5% skim-milk 0.3% TritonX-100 buffer, exposed to claudin-5 rabbit polyclonal Ab [1:500, 1 h, room temperature (RT)], washed 3 times in PBS 0.01% TritonX-100, incubated in appropriate secondary Ab (1 h, RT), washed 3 times in PBS 0.01% TritonX-100, and fixed again with 1% paraformaldehyde (PAF) for 20 min at RT.
After 5 min wash with PBS 0.01% TritonX-100, the allantoises were blocked in 2.5% skim-milk 0.3% TritonX-100 buffer, exposed to PECAM Ab (5 μg/ml, 1 h, RT), washed 3 times in PBS 0.01% TritonX-100, incubated in appropriate secondary Ab (1 h, RT), washed 3 times in PBS 0.01% TritonX-100 and mounted with Mowiol Mounting Medium (Calbiochem, La Jolla, CA). Stained allantoises were analysed by scanning confocal microscopy.

FoxO luciferase assay. VEC positive cells, wild type or infected with the indicated constructs, were seeded at 45.000 cells/cm^2; VEC null cells were seeded at 55.000 cells/cm^2 in 6-well plates, in complete culture medium without penicillin/streptomycin. The day after, cells were transiently transfected with 1 μg/well of pCMV-βGAL expressing vector and 3 μg/well of 6xDBE-luc,

© 2008 Macmillan Publishers Limited. All rights reserved.

pSODLUC or pSODLUC-mut plasmid using 5 µl/ml LipofectAMINE 2000 (Invitrogen) or 10µl/well of ArrestIN (Invitrogen) in OptiMEM (Invitrogen) according to the manufacturer's instructions. After 5 h of incubation, cells were rinsed and further incubated in fresh complete culture medium. 48 h after transfection cells were washed twice with MCDB 131 and starved for 24 h. Cells were then lysed in lysis buffer (BD Biosciences, San Jose, CA), and luciferase activity was measured using the Enhanced Luciferase Assay Kit (BD Biosciences) according to the manufacturer's instructions with a luminometer (Lumat LB 9501; Berthold, Bad Wildbad, Germany). βGAL activity was used as normalizer for transfection efficiency.

TOP/FOP assay. The assay was carried out using standard technique described previously[56]. Briefly, cells were plated in 24-well plates to form 60 to 80% confluent cultures at time of transfection. 24 h after seeding, cells were transfected using the LipofectAMINE PLUS method (Invitrogen), in triplicate, in accordance with the manufacturer's instructions.
To normalize for transfection efficiency a pCMV-βGAL plasmid was co-transfected. Luciferase activity was assayed 24 h after transfection, using a dual-luciferase reporter assay system (Promega, Madison, WI).
Tcf-β-catenin-mediated gene transcription was defined by the ratio of TOP-TK-LUC/FOP-TK-LUC luciferase activities, where the βGAL activity of the internal control reporter pCMV-βGAL was used to correct for differences in transfection efficiency.

Immunofluorescence microscopy. Cells were cultured in 35 mm diameter petri dishes. For β-catenin stainings of Fig. 5b, 5e and 6b cells were fixed with 4% PAF for 20 min at RT. For all other stainings cells were fixed and permeabilized in methanol at -20°C for 5 min. Fixed cells were incubated for 30 min in a blocking solution: for JAM A, β-catenin and claudin-5 stainings blocking buffer was PBS 2.5% skim-milk 0.3% TritonX-100, for all other stainings blocking buffer was PBS

© 2008 Macmillan Publishers Limited. All rights reserved.

2% BSA. Cells were then incubated for 1 h at RT with primary Abs diluted in blocking buffer. Appropriate secondary Abs were applied on cells for 45 min at RT.

Samples were observed under a fluorescence microscope (DMR; Leica, Solms, Germany) using 63X or 100X lenses. Images were captured using a charge-coupled camera (model 3; Hamamatsu, Hamamatsu City, Japan) before processing through Adobe Photoshop. Only adjustments of brightness and contrast were used in the preparation of the figures. For comparison purposes, different sample images of the same antigen were acquired under constant acquisition settings.

Confocal microscopy was performed with a Leica TCS SP2 AOBS confocal microscope equipped with violet (405 nm laser diode), blue (Argon, 488 nm), yellow (561 nm Solid State Laser) and red (633 nm HeNe Laser) excitation laser lines. Image acquisition was performed using a 63X/1.4 NA oil immersion objective (HCX PL APO 63X Lbd Bl, Leica) and with spectral detection bands and scanning modalities optimized for removal of channels cross talk. Leica Confocal Software and ImageJ 1.33 (W. Rasband, NIH, Bethesda, USA) were employed for data analysis.

To quantify the flurescence signal from confocal microscopy images of allantoises, ImageJ 1.33 was used to draw a fixed area containing PECAM-stained endothelial cells. The junctional fluorescence density of claudin-5 was determined from images of 2 allantoises per each genotype, quantified with at least 20 areas per field. Microsoft Excel was used to determine mean integrated fluorescence density values and average deviation for each genotype.

Western blot analysis. Total proteins were extracted by solubilising cells in boiling Laemmli buffer [2.5% SDS and 0.125 M Tris-HCl (pH 6.8)]. Lysates were incubated for 5 min at 100°C to allow protein denaturation and then spinned for 5 min at 13,200 rpm to discard cell debris. The supernatants were collected and the concentration of protein was determined using a BCA™ Protein Assay Kit (Pierce) according to manufacturer's instructions. Equal amount of proteins were loaded on gel and separated by SDS-PAGE, transferred to a Protran Nitrocellulose Hybridization Transfer Membrane 0.2 μm pore size (Whatman, Kent, UK) and blocked for 1 h at RT in 1X TBST

© 2008 **Macmillan Publishers Limited. All rights reserved.**

[150 mM NaCl, 10 mM Tris-HCl (pH 7.4), and 0.05% Tween]-powdered milk. The membranes were incubated O/N at 4°C or 1 h at RT, in primary Abs diluted in 1X TBST-5% BSA. Next, they were rinsed 3 times with 1X TBST for 5 min each and incubated for 1 h at RT with horseradish peroxidase-linked secondary Abs (diluted in 1X TBST-5% BSA). Membranes were rinsed 3 times with TBST for 5 min each, and specific binding was detected by the enhanced chemiluminescence (ECL) system (Amersham Biosciences) using HyperfilmTM (Amersham Biosciences). The molecular masses of proteins were estimated relative to the electrophoretic mobility of co-transferred prestained protein marker, Broad Range (Cell Signaling Technology, Beverley, MA).

Paracellular tracer flux analysis. For the paracellular tracer flux analysis performed on siRNA-transfected cells, VEC positive cells were seeded in 35 mm diameter petri dishes to form 90% confluent cultures at time of tansfection. 24 h after seeding, cells were transfected with siRNAs using LipofectAMINE 2000 method according to the manufacturer's instructions. The next day cells were detached, seeded on 6.5 mm diameter Transwell Permeable Supports (pore size 0.4 μm) and cultured in complete culture medium for 48 h. For the paracellular tracer flux analysis performed on cells infected with FKHR-TM adenoviral vector, confluent VEC positive cells were infected directly on Transwell Permeable Supports and cultured for 72 h in complete culture medium before assaying permeability. Next, FITC-dextran (38 kDa) was added to the medium of the transwell apical compartment at a concentration of 1 mg/ml. At different times of incubation, a 50 μl aliquot of the medium was collected from the basal compartment, and the paracellular tracer flux was measured as the amount of FITC-dextran in the medium using the fluorometer Wallac Victor^3 1420 multilabel counter (Perkin Elmer).

Antibodies and chemicals. Abs used in this study were: claudin-5 mouse monoclonal (Zymed, San Francisco, CA); claudin-5 rabbit polyclonal (from H. Wolburg, Institute of Pathology, University of Tubingen, Tubingen, Germany); active-β-catenin mouse monoclonal (anti-ABC) (Upstate-

© 2008 Macmillan Publishers Limited. All rights reserved.

Millipore, Temecula, CA); β-catenin mouse monoclonal (BD Biosciences); FKHR (H-128) rabbit polyclonal and VE-cadherin goat polyclonal (Santa Cruz Biotechnology, Santa Cruz, CA); FoxO1 rabbit polyclonal, phospho-FoxO1 (Ser 256) rabbit polyclonal, phospho-FoxO1 (Thr 24) rabbit polyclonal, AKT rabbit polyclonal, AKT1 rabbit monoclonal, phospho-AKT (Thr 308) rabbit polyclonal, ERK rabbit polyclonal and phospho-ERK (Thr 202, Tyr 204) rabbit polyclonal (Cell Signaling Technology); HA-tag mouse monoclonal (BabCo, Richmond, CA), Myc-tag mouse monoclonal (from internal service); ZO-1 rabbit polyclonal (Zymed); cingulin rabbit polyclonal (Zymed); VE-cadherin mouse monoclonal (BV9) (produced in our laboratory[57]); PECAM rat monoclonal (Mec 13.3)[58]; JAM A rat monoclonal (BV12)[59]; JAM B 829 rabbit polyclonal and JAM C 501 rabbit polyclonal (from B. Imhof, University of Geneva, Geneva, Switzerland); NP-95 rabbit polyclonal (from F. Nicassio and P.P. Di Fiore, IFOM-Firc Institute of Molecular Oncology, Milan, Italy); α-tubulin mouse monoclonal, vinculin mouse monoclonal and Flag-tag mouse monoclonal (Sigma); DC101 Ab (obtained through ImClone, New York City, NY).

The following reagents were used in this study: AKT inhibitor (1L-6-Hydroxymethyl-*chiro*-inositol2-(R)-2-O-methyl-3-O-octadecylcarbonate) (Calbiochem); pan-caspase inhibitor zVAD-fmk (Bachem, Bubendorf, Switzerland); lithium chloride (Sigma); sodium chloride (Carlo Erba Reagenti, Milan, Italy); PI3K inhibitor LY 294002 (Cell Signaling Technology); VEGF-A (PeproTech, Rocky Hill, NJ); Sunitinib malate (SU11248) (from F. Bertolini, European Institute of Oncology, Milan, Italy); leptomycin B (Sigma).

© 2008 **Macmillan Publishers Limited. All rights reserved.**

REFERENCES

51. Balconi,G., Spagnuolo,R., & Dejana,E. Development of endothelial cell lines from embryonic stem cells: A tool for studying genetically manipulated endothelial cells in vitro. *Arterioscler. Thromb. Vasc. Biol.* **20**, 1443-1451 (2000).

52. Brault,V. *et al.* Inactivation of the beta-catenin gene by Wnt1-Cre-mediated deletion results in dramatic brain malformation and failure of craniofacial development. *Development* **128**, 1253-1264 (2001).

53. Navarro,P. *et al.* Catenin-dependent and -independent functions of vascular endothelial cadherin. *J. Biol. Chem.* **270**, 30965-30972 (1995).

54. Corada,M. *et al.* A monoclonal antibody to vascular endothelial-cadherin inhibits tumor angiogenesis without side effects on endothelial permeability. *Blood* **100**, 905-911 (2002).

55. Dong,Q.G. *et al.* A general strategy for isolation of endothelial cells from murine tissues. Characterization of two endothelial cell lines from the murine lung and subcutaneous sponge implants. *Arterioscler. Thromb. Vasc. Biol.* **17**, 1599-1604 (1997).

56. Hagen,T., Di,D.E., Culbert,A.A., & Reith,A.D. Expression and characterization of GSK-3 mutants and their effect on beta-catenin phosphorylation in intact cells. *J. Biol. Chem.* **277**, 23330-23335 (2002).

57. Corada,M. *et al.* Monoclonal antibodies directed to different regions of vascular endothelial cadherin extracellular domain affect adhesion and clustering of the protein and modulate endothelial permeability. *Blood* **97**, 1679-1684 (2001).

© 2008 **Macmillan Publishers Limited. All rights reserved.**

58. Vecchi,A. *et al.* Monoclonal antibodies specific for endothelial cells of mouse blood vessels. Their application in the identification of adult and embryonic endothelium. *Eur. J. Cell Biol.* **63**, 247-254 (1994).

59. Cera,M.R. *et al.* Increased DC trafficking to lymph nodes and contact hypersensitivity in junctional adhesion molecule-A-deficient mice. *J. Clin. Invest* **114**, 729-738 (2004).

© 2008 **Macmillan Publishers Limited. All rights reserved.**